Estuaries and Coasts
September 2022, Volume 46, Pages 128-148
https://doi.org/10.1007/s12237-022-01121-6
https://archimer.ifremer.fr/doc/00793/90529/

Seasonal, Diurnal, and Tidal Variations of Dissolved Inorganic Carbon and pCO2 in Surface Waters of a Temperate Coastal Lagoon (Arcachon, SW France)

Polsenaere Pierre [1, 2, *], Delille Bruno [3], Poirier Dominique [1], Charbonnier Céline [1], Deborde Jonathan [1, 2], Mouret Aurélia [1, 4], Abril Gwenaël [1, 5, 6]

[1] Laboratoire Environnements et Paléoenvironnements Océaniques et Continentaux (EPOC), CNRS-UMR 5805, Université de Bordeaux, Bordeaux, France
[2] IFREMER, Littoral, Laboratoire Environnement et Ressources des Pertuis Charentais (LER-PC), BP133, 17390, La Tremblade, France
[3] Département d'Astrophysique, Géophysique Et Océanographie, Unité Océanographie Chimique, Université de Liège, Allée du 6 Août, 17-Bât. B5 4000, Liège, Belgium
[4] UMR 6112 LPG-BIAF Recent and Fossil Bio-Indicators, Angers University, 2 Bd Lavoisier, F-49045, Angers, France
[5] Laboratoire de Biologie des Organismes et Écosystèmes Aquatiques (BOREA), UMR CNRS 8067, Muséum National d'Histoire Naturelle, 61 rue Buffon, 75231, Paris cedex 05, France
[6] Programa de Biologia Marinha e Ambientes Costeiros, Universidade Federal Fluminense, Outeiro São João Batista s/n, 24020015, Niterói, RJ, Brazil

* Corresponding author : Pierre Polsenaere, email address : Pierre.Polsenaere@Ifremer.fr

Abstract :

We report on diurnal, tidal, and seasonal variations of dissolved inorganic carbon (DIC), water partial pressure of CO2 (pCO2), and associated water–air CO2 fluxes in a tidal creek of a temperate coastal lagoon with 70% of intertidal flats, during eight tidal/diurnal cycles and two consecutive years covering all seasons. Surface waters of the lagoon were always slightly oversaturated in CO2 with respect to the atmosphere with an average pCO2 value of 496 ± 36 ppmv. Seasonally, subsurface water pCO2 values were controlled by both temperature and biological/tidal advection effects that compensated each other and resulted in weak annual variations. High-resolution temporal pCO2 records reveal that the highest fluctuations (192 ppmv) occurred at the tidal/diurnal scale as a result of biological activity, advection from the tidal flat, and porewater pumping that all contributed to water pCO2 and carbonate chemistry variations. Total alkalinity (TA) versus salinity plots suggest a net production of alkalinity in the lagoon attributed to benthic carbonate dissolution and/or anaerobic degradation of organic matter. We specifically highlighted that for the same salinity range, during flooding, daytime pCO2 were generally lower than nighttime pCO2 values because of photosynthesis, whereas during ebbing, daytime pCO2 were higher than nighttime pCO2 values because of heating. Waters in the lagoon were a relatively weak CO2 source to the atmosphere over the year compared to other estuarine and lagoon waters elsewhere, and to sediment-air fluxes measured simultaneously by atmospheric Eddy Covariance (EC) in the Arcachon lagoon. Because of low values and small variations of the air-sea pCO2 gradient, the variability of fluxes calculated using the piston velocity parameterization was greatly controlled by the wind speed at the diurnal and, to a lesser extent, seasonal time scales. During the emersion, the comparison of these pCO2

data in the tidal creek with EC fluxes measured 1.8 km away on the tidal flat suggests high heterogeneity in air-sea CO2 fluxes, both spatially and at short time scales according to the inundation cycle and the wind speed. In addition to tidal pumping when the flat becomes emerged, our data suggest that lateral water movement during the emersion of the flat generates strong spatial heterogeneity in water–air CO2 flux.

Keywords : Coastal zone, Dissolved inorganic carbon, Water pCO2, Water–air CO2 fluxes, Tidal, diurnal, seasonal variations, Physical, biological, chemical processes

1. Introduction

Coastal zones represent key systems in biogeochemical cycle couplings between land, oceans and the atmosphere, processing considerable amounts of matter, energy and nutrients (Borges et al. 2005; Cole et al. 2007; Cai 2011). Despite its relatively modest surface area (7 % of the global ocean surface), the coastal zone accounts for 14-30 % of all oceanic primary production and 90 % of sedimentary organic carbon mineralization (Gattuso et al. 1998; Mantoura et al. 1991; Pernetta and Milliman 1995). Carbon fluxes within and between coastal subsystems and their alteration by climate and anthropogenic changes are substantial. It is essential to understand and accurately account for the factors regulating these fluxes and how they affect the ocean and global carbon budgets (Bauer et al. 2013).

The coastal ocean consists of different but tightly connected ecosystems including estuaries, tidal wetlands, lagoons and the continental shelf. Global CO_2 emissions from estuaries have been estimated at 0.2-0.4 Pg yr^{-1} (Cai 2011; Borges and Abril 2011; Borges et al. 2005; Laruelle et al. 2010), with fluxes disproportionally high in comparison with their global ocean area portion (near 0.2 %). To the contrary, other coastal systems such as tidal wetlands and continental shelves fix 0.55 and 0.25 Pg yr^{-1} of atmospheric CO_2 respectively (Bauer et al. 2013). The spatiotemporal heterogeneity and complexity of coastal systems in terms of carbon processes and fluxes make difficult to precisely quantify each sub-system's carbon balance. For instance, carbon fluxes in tidal systems such as estuaries and small deltas are relatively well characterized (Laruelle et al. 2010; Borges and Abril 2011; Chen et al. 2013). To the contrary, other systems such as fjords, lagoons and marine embayments are neglected despite a large relative surface among coastal systems, a generally high net primary production and a strong sensitivity to eutrophication phenomenon (Kjerfve 1985; Caumette et al. 1996; Koné et al. 2009; Polsenaere et al. 2012a; Cotovicz et al. 2015). As a consequence, carbon flux measurements are needed for an accurate estimate of global and regional carbon budgets.

In coastal ecosystems, dissolved inorganic carbon (DIC) concentrations, and particularly partial pressures of CO_2 (pCO_2) are driven by several thermodynamic and biotic factors, induced by river water inputs, tidal exchanges, mixing of water masses, photosynthesis and aerobic/anaerobic degradation of organic matter, precipitation/dissolution of calcium carbonate, benthic/pelagic couplings and air-water exchanges (Cai 2011; Gazeau et al. 2004; Cotovicz et al. 2015; Ribas-Ribas et al. 2011). Efforts have been made to understand the seasonal and inter-annual processes affecting carbon system dynamics over coastal ecosystems (Yates et al. 2007). Seasonal measurements of the carbonate system parameters (pCO_2, Total Alkalinity, DIC, and/ or pH) have been performed for instance across salinity gradient transects or strategically located stations along lagoon channels or estuaries (Frankignoulle et al. 1996; Cai et al. 1999; Koné et al. 2009; Ribas-Ribas et al. 2011; Burgos et al. 2018; Wang et al. 2018; Vaz et al. 2019). The influence of smaller-scale rhythms (tidal and diurnal variations) on seasonal and annual carbon dynamics and budgets has also been studied through direct diurnal cycles for instance over east monsoon coastal systems and subtropical bays (Dai et al. 2009; Yates et al. 2007), temperate sea, lagoon, estuary, river, channel and creek (Saderne et al. 2013; Bozec et al. 2011; Borges and Frankignoulle 1999; Ribas-Ribas et al. 2013; Burgos et al. 2018), sub-Antarctic island coastal waters (Delille et al. 2009), tropical and equatorial mangrove waters (Maher et al. 2013; Bouillon et al. 2007; Borges et al. 2003) and continental and subtropical saltmarsh and marsh-dominated estuary systems (Wang and Cai, 2004; Wang et al. 2016; Wang et al. 2018). For instance, in a tidal creek among the Duplin River salt marsh-estuary coastal ecosystem (Georgia, USA), Wang et al. (2018) measured strong seasonal and tidal/diurnal pCO_2 variations with values ranging from 500 ppmv at high tide to 4000 ppmv at low tide and to 1600 ppmv at high tide to 12,000 ppmv at low tide during coldest and warmest months, respectively. Horizontal advection with river water entrance to the creek at high tide was mentioned to explain lower measured values. To the contrary, for higher values observed

at low tide, creek bank pore-water drainage associated to tidal pumping process, as observed over mangroves or wetlands (Maher et al. 2013; Neubauer and Anderson 2003) was highlighted (Wang et al. 2018). Over tidally-influenced shallow systems, all these processes are generally but differently involved and can in turn significantly and specifically influence atmospheric CO_2 fluxes.

CO_2 fluxes at the water-air interface can be measured directly using the Eddy Covariance (Zemmelink et al. 2009; Polsenaere et al. 2012a), floating chambers (Frankignoulle et al. 1998) or be calculated from water pCO_2 measurements and a given gas transfer velocity. CO_2 flux computations can be subject to large uncertainties because of the difficulty in accurately assessing the gas transfer velocity (Raymond and Cole 2001, Vachon et al. 2010). This bias is potentially more important when the water-air CO_2 gradient is small. Diurnal and tidal variations in water pCO_2 of dynamic coastal ecosystems can even add uncertainties on air-sea CO_2 flux estimations. For example, in the Guadalquivir estuary, Ribas-Ribas et al. (2013) observed pCO_2 values fluctuating from source to sink over the same tidal cycle.

In the present study we report tidal, diurnal and seasonal dynamics of inorganic carbon and associated air-sea CO_2 fluxes in a tidal creek of the temperate coastal Arcachon lagoon (SW France). The lagoon is a typical tidal flat of the French Atlantic coast subjected to both marine and continental influences. A complex channel and tidal creek waters network drains the tidal flat during ebb tides. Tidal pumping through anoxic pore-water seeping from mud sediments to tidal creek waters is an important component of the biogeochemical functioning of the lagoon in terms of nutrient dynamics (Deborde et al., 2008a). In this paper, DIC parameters and associated water-air CO_2 fluxes as estimated based on several *in situ* tidal/diurnal cycles (six 24-hour and two 12-hour cycles) carried at different seasons during two years (2008 and 2009) are presented. We describe and explain small-scale (diurnal and tidal) and seasonal pCO_2 variability along with relevant environmental controls in studied tidal creek waters. We

compute air-sea CO_2 fluxes, and discuss associated variability according to small (diurnal and tidal) and seasonal scales and also methodology from coastal regional/global carbon budgets point of view. The computed water-air CO_2 fluxes estimated during these tidal/diurnal cycles are also compared with those measured in summer 2008 by atmospheric Eddy Covariance (EC) over the tidal flat (Polsenaere et al. 2012a).

2. Materials and Methods

2.1. Study area

The Arcachon bay is a temperate macro-tidal lagoon of 174 km^2 on the southwestern Atlantic coast of France (44°40' N, 01°10' W) (Fig. 1). Several studies have focused on the system in particular its hydrodynamics through modelling simulations (Plus et al. 2009; Fauvelle et al. 2018); Zostera seagrass meadow dynamic (Auby and Labourg 1996; Plus et al. 2010; Cognat et al. 2018) and relationships with sediment hydrodynamics or redox status (Ganthy et al. 2013; Delgard et al. 2013; Deborde et al. 2008a,b); nutrient and carbon dynamics and export from the Arcachon catchment through *in situ* adapted sampling and modelling strategies (Auby et al. 1994; Rimmelin et al. 1998; Canton et al. 2012; Polsenaere et al. 2012b; Polsenaere and Abril 2012); and in terms of benthic and pelagic primary production measurements through various *in situ,* laboratory and modelling approaches (Polsenaere et al. 2012a; Migné et al. 2016; Glé et al. 2008; Plus et al. 2015).

This triangle-shaped bay is surrounded by the coastal plain of the *Landes de Gascogne*, and communicates with the Atlantic Ocean through a narrow channel 8 km in length (Fig. 1). With a mean depth of 4.6 m, the shallow lagoon presents semi-diurnal tides with amplitudes varying from 0.8 to 4.6 m (Plus et al. 2009). During a tidal cycle, the flat exchanges approximately 264 $\times 10^6$ m^3 and 492 $\times 10^6$ m^3 of water with the ocean, respectively during average neap and spring tides. The flushing time of the lagoon ranges between 12.4 and 17.4 days in winter and summer

respectively (Plus et al. 2009). Water temperatures in the lagoon vary from 6 °C in winter to 22.5 °C in summer, and water salinity varies from 22 to 35 according to freshwater input variations during the year.

The flats are tidally submerged by relatively saline waters, and receive moderate amounts of freshwater with an annual input of 813×10^6 m^3 (1.8×10^6 m^3 at each tidal cycle), of which 8 % is from groundwater, 13 % is from rainfall and 79 % is from rivers and small streams (Rimmelin et al. 1998). In total, the carbon export from the watershed to the Arcachon lagoon was estimated at 15,870 t C yr^{-1} or 6 t C km^{-2} yr^{-1}, mostly in the form of dissolved organic carbon (DOC) (35 %), DIC (24 %) as excess CO_2 and $DIC_{equilibrium}$ (i.e. the theoretical DIC concentration at the atmospheric equilibrium), and dissolved CO_2 rapidly lost as degassing to the atmosphere (34 %) (Polsenaere et al. 2012b). Tidal pore-water drainage at low tide is not documented for carbon, but contributes to respectively 55 and 15 % of the dissolved inorganic phosphate (DIP) and nitrate (DIN) input to the lagoon waters (Deborde et al. 2008a).

The lagoon surface is composed of 57 km^2 of channels (33 % of the lagoon surface area), with a maximum depth of 25 m at the mouth of the lagoon. These channels drain a large muddy tidal flat of 117 km^2 (67 % of the lagoon). *Zostera noltei* seagrass beds are particularly extensive and colonize up to 60 % of this intertidal area (i.e. 70 km^2) between −1.9 m and +0.8 m relative to local Mean Sea Level (Amanieu, 1967). Annual mean net primary production of *Zostera noltei* expressed as carbon fixation was estimated at 362.9 ± 88.1 t C km^{-2} yr^{-1} (Ribaudo et al. 2017). Polsenaere et al. (2012a) and Migné et al. (2016) gave annual values of the same order of magnitude through atmospheric EC and benthic chamber measurements with 456 and 263 t C km^{-2} yr^{-1} respectively. However, seagrass beds in the lagoon declined by 33 % since the end of the 80's whereas the exact causes remain unclear, leading to a C fixation decline from 24846 ± 6030 t C yr^{-1} (1989) to 16564 ± 4020 t C yr^{-1} (2007) (Plus et al. 2009; Plus et al. 2015; Ribaudo et al. 2017). The microphytobenthic (MPB) communities also represent a significant proportion

of the total benthic primary production, which is estimated at between 104-114, 628 and 788 t C km^{-2} yr^{-1} (Auby personal communication; Polsenaere et al. 2012a; Migné et al. 2016). Together, these two categories of benthic primary production represent more than half of the total primary production of the flat. Annual integrated phytoplankton primary production has been estimated at 103 t C km^{-2} yr^{-1} which could represent 30 % of the total primary production of the lagoon and places Arcachon within the low to moderate phytoplankton primary production systems (Glé et al. 2008). Microphythobenthic resuspension is also supposed to significantly contribute to planktonic production in Arcachon as highlighted by Savelli et al. (2019) on the Brouage mudflat of the Marennes-Oléron Bay up North along the French Atlantic coast with a 43 % resuspended MPB primary production at this location. The presence of circular tidal pools on the flat also contributes to the biogeochemical functioning of Arcachon bay especially at tidal and diurnal scales (Rigaud et al. 2018) through large spatio-temporal variations in water temperature and irradiance influencing MPB activity and benthic oxygen, nutrients, and reduced compound fluxes.

Finally, net CO_2 fluxes between the lagoon and the atmosphere measured at the ecosystem scale by atmospheric EC generally showed small negative (influx) and positive (efflux) values (-13 μmol m^{-2} s^{-1} for influxes and 19 μmol m^{-2} s^{-1} for effluxes). Emersion during the day was almost always associated with a net uptake of atmospheric CO_2 due to an enhanced benthic primary production at low tide. In contrast, during immersion (day and night) and emersion at night, CO_2 fluxes were positive, negative or close to zero, depending on the season and the study site (Polsenaere et al. 2012a).

2.2. Sampling strategy and laboratory analysis

In total, six 24-hour cycles (April, July, September 2008, and April, June and September 2009) and two 12-hour cycles (November 2008 and January 2009) were carried out in a subtidal creek at the centre of the lagoon (Fig. 1). For each cycle, water height (H), salinity (S), temperature

(T), partial pressure of CO_2 in the water (pCO_2), total alkalinity (TA) and dissolved inorganic carbon isotopic ratio (δ^{13}C-DIC) were measured at the subsurface (0.5 m depth). T and S were measured every minute with an YSI multiparameter probe on board and H was measured every hour by the SHOM (Service Hydrographique et Océanographique de la Marine) at Arcachon (Eyrac pier, 44°39.9001'N 01°09.8130'W). Before each cycle, the salinity (conductivity) sensor was checked and calibrated with 10 and 50 mS cm^{-1} solutions. Water pCO_2 was measured every minute with a marble-type equilibrator system (Frankignoulle et al. 2001; Polsenaere et al. 2012b). An Infra-Red Gas Analyzer (LI-COR, LI-820) was used to measure the pCO_2 in dry air equilibrated with seawater. The LI-820 was calibrated at the laboratory one day before the field experiment using three gas standards of 0, 500 ± 10 ppm and 2959 ± 59 ppm. The equilibrator consists of a Plexiglas cylinder (height: 90 cm, diameter: 16 cm) that is filled with marbles to increase the exchange surface area. Water pumped by a peristaltic pump (Masterflex, 1 L min^{-1}), runs from the top to the bottom of the equilibrator, and air is pumped upwards (1 L min^{-1}). The pCO_2 of air equilibrates with the pCO_2 of water and is then measured by the LI-COR after being dried by a Dierite grain tube. Response time of the equilibrator as determined in the laboratory is shorted than 5 minutes (Cotovicz et al. 2016).

Discrete water samples were also taken every hour of the tidal cycle for TA and δ^{13}C-DIC in the channel subsurface waters by using a 5L Niskin sampler. Total alkalinity (TA) was measured by titration with HCl 0.1 N on 100 mL filtered samples and was calculated by a Gran function linearisation (Gran 1952) between pH 4.2 and 3. The reproducibility between the measures was better than ±5 µmol kg^{-1}. Accuracy of TA measurements was checked on regular titrations of a secondary standard of 0.2 µm filtered seawater with a well-known TA concentration, previously calibrated by comparison with a standard from Scripps Institution of Oceanography. The δ^{13}C-DIC measurements were made following Gillikin and Bouillon (2007). In 100 mL vials that were filled to the top, a headspace was first created with Helium

gas to obtain a volume of approximately 20 % of the total volume of the vial. Then, 0.3 mL of warm 85 % phosphoric acid was added to transform the carbonate forms into CO_2. To ensure gas equilibration, the vials were shaken and placed upside down for 1.5 h. Measurements were performed by coupling an elemental analyzer (EA; Carlo Erba NC2500) to an Isotope Ratio Mass Spectrometer (IRMS; Micromass Isoprime) equipped with a manual gas injection. We injected 3 mL of headspace gas from the vial headspace. δ^{13}C-DIC was calibrated against a laboratory standard (45 mg of Na_2CO_3 were dissolved in a sealed vial flushed with He gas, with 3 mL of warm 85 % phosphoric acid H_3PO_4). This standard had been calibrated against a certified standard (NBS19, -1.96 ‰) using a dual-inlet IRMS. The isotopic value of the standard Na_2CO_3 was -4.5 ± 0.2 ‰. Finally, the equation of Miyajima et al. (1995) was applied to correct for the isotopic fractionation of the CO_2 between the headspace and the water phase and to calculate the δ^{13}C of the total DIC. The repeatability was approximately ±0.1 ‰ between samples. The stable isotopic composition of DIC (δ^{13}C-DIC) varies over a large range in terrestrial and coastal waters since carbon reservoirs that act as a source of DIC (soil, groundwater, bedrocks and atmosphere) have distinct isotopic signatures (Yang et al. 1996). The δ^{13}C of atmospheric CO_2 is about -7.5 ‰, whereas carbonate rocks have a δ^{13}C of about 0 ‰ (Mook et al. 1983). In a system where soil CO_2 is primarily derived from decomposition of plant organic matter, the CO_2 produced has a $\delta^{13}C–CO_2$ value close to the initial substrate (i.e., -30 to -24 ‰ int the case of C3 plants and -16 to -10 ‰ in the case of C4 plants). Aquatic primary production, in contrast, tends to increase δ^{13}C-DIC and generate strong diel variations (Parker et al. 2005). Finally, gas exchange along subsurface waters generates an isotopic equilibration with the atmosphere and makes the δ^{13}C-DIC less negative.

2.3. Calculations and statistical analysis

Dissolved inorganic carbon (DIC) concentrations and species (bicarbonate HCO_3^- and carbonate CO_3^{2-} ions) were calculated from the measured salinity, temperature, pCO_2 and TA using the carbonic acid constants sets from by Mehrbach et al. (1973) as modified by Dickson and Millero (1987), the borate acidity constant from Lee et al. (2010), the K_{HSO4} constant from Dickson (1990) and the CO_2 solubility coefficient of Weiss (1974). The CO_2 System Calculation program (version 2.1.) developed by Lewis and Wallace (1998) performed all calculations.

Seasonal temperature ($TpCO_2$) versus non-temperature ($NpCO_2$) effects on measured water pCO_2 during the eight tidal cycles were studied applying equations from Takahashi et al. (2002) as follows:

$$TpCO_2 = pCO_{2mean} \times \exp[0.0423(T_{obs} - T_{mean})] \quad (1)$$

$$NpCO_2 = pCO_{2obs} \times \exp[0.0423(T_{mean} - T_{obs})] \quad (2)$$

Where pCO_{2obs}, T_{obs}, pCO_{2mean}, T_{mean} are respectively the measured pCO_2, temperatures at each time step and the annual mean pCO_2 and temperature calculated across the whole measured dataset. $TpCO_2$ indicates the pCO_2 variations around the mean pCO_2 that would be expected only from temperature fluctuations that occurred over the sampling period (2008-2009). $NpCO_2$ represent pCO_2 variations due to biological activity or non-temperature effects (advection, tidal pumping and benthic-pelagic coupling). The constant 0.0423 corresponds to the temperature effect on pCO_2 in isochemical conditions ($q\ln pCO_2/qT$), i.e. +4.23 % $°C^{-1}$.

Gas transfer velocities (k_{600}) and air-sea CO_2 fluxes for the eight tidal cycles were computed each hour at high-tide day and night periods. Wind speed values normalized to a 10 meters height (U_{10}) values were computed from wind speed values measured at 9 meters high by the Lège-Cap Ferret Meteo-France station (44°37.900'N 01°14.900W, 12.5 km far from the 24-H site, Fig. 1) using the Amorocho and DeVries (1980) equation. Gas transfer velocities (k) were estimated according to parameterizations of Wanninkhof et al. (1992), Raymond and Cole

(2001) and Abril et al. (2009), noted W92, RC01 and A09, respectively. The W92 equation has been proposed for oceanic water, whereas the RC01 and A09 equations were developed for estuarine waters. For the latter equation, hourly suspended particulate matter (SPM) concentrations measured during every cycle (data not shown) and bottom water velocity currents estimated with the hydrodynamic model from Ifremer (MARS3D, Lazure and Dumas, 2008) were used. Air-sea CO_2 fluxes were then calculated from k, water and air pCO_2 values. The gas transfer coefficients normalized to a Schmidt number of 600 (k_{600}) estimated with the three parameterizations were converted to the gas transfer velocity of CO_2 (k) at *in situ* temperature and salinity following the procedure of Jähne et al. (1987). Air-water CO_2 fluxes were estimated using the formulation as followed:

$$F_{CO2}=\boldsymbol{\alpha} k \Delta pCO_2 \quad (3)$$

where F_{CO2} is the vertical CO_2 exchange at the air-water interface, $\boldsymbol{\alpha}$ is the CO_2 solubility coefficient (Weiss 1974), k is the gas transfer velocity, and ΔpCO_2 is the gradient between water pCO_2 measured by the equilibrator and air pCO_2 set to a mean value of 390 ppm according to simultaneous Eddy Covariance (EC) measurements done in the lagoon (44°42.9858'N 01°08.6160'W, 1.829 km far from the 24-H site, Fig. 1) in 2008 and 2009 (Polsenaere et al. 2012a). For comparison, U_{10} and air-sea CO_2 flux values obtained in July 2008 from simultaneous EC measurements (Polsenaere et al. 2012a) and water carbon parameters (pCO_2) during the July 2008 cycle are also presented.

Data post-processing (graphs and statistics) was performed using the GraphPad Prism version 6.00 software (La Jolla California USA, www.graphpad.com). The Shapiro-Wilk test was used to test the normality of the data (p-value below 0.05). Due to non-normality of our data, Mann-Whitney and Kruskal-Wallis (p-value below 0.05) were performed to detect significant differences in carbon and associated parameters between tidal/diurnal cycles (seasons) and also across diurnal and tidal rhythms (emersion around low tide during the day (LT/Day), emersion

at night (LT/Night), immersion around high tide during the day (HT/Day) and immersion at night (HT/Night)) (emersion and immersion periods last during 4 and 8 hours twice per day in the Arcachon lagoon). The Dunn's post-hoc multiple comparisons' test to Kruskal-Wallis was chosen to detect significant differences among groups.

3. Results

3.1. Water pCO_2 and associated parameter temporal variations

3.1.1. At the seasonal time scale

In 2008/09 at our 2.5 meter deep (on average, hydrographic zero) subtidal creek in the Arcachon lagoon, water temperatures averaged 17.7 ± 4.2 °C over the years 2008 and 2009 and ranged between 8.9 ± 0.4 °C in January 2009 and 22.2 ± 0.6 °C in July 2008 (Table 1, Fig. 2). Water mean salinity value was 30.5 ± 3.4 with a particularly low mean value measured in January 2009 (Table 1, 23.2 ± 1.5, Fig. 3).

Bicarbonates (HCO_3^-), carbonates (CO_3^{2-}) and the sum of dissolved CO_2 and carbonic acid H_2CO_3 concentrations (CO_2^*) represented respectively 91 to 95 %, 3 to 8 % and about 1 % of the whole DIC (data not shown). TA values followed DIC patterns with a lowest mean value of 1.646 ± 0.086 mmol kg^{-1} in January 2009 and a highest mean value 2.255 ± 0.021 mmol kg^{-1} in September 2008 (Fig. 3, Table 1). δ^{13}C-DIC mean values were close to 0 ‰ and ranged between -1.1 ± 1.1 ‰ in April 2008 (minimum values in winter/spring) and -0.2 ± 0.2 ‰ in June 2009 (maximum values in summer/autumn). Particularly low negative values up to -3.7 ‰ were measured in April 2008 (Table 1, Fig. 3). Over the whole studied period, global significant and positive TA, DIC and δ^{13}C-DIC values versus salinity values were obtained (TA=0.05143*S + 0.5079, R^2: 0.88; DIC=0.03815*S + 0.7594, R^2: 0.82; δ^{13}C-DIC=0.08697*S - 3.284, R^2: 0.15; $p<0.0001$, Fig. 4a, c, d). At each cycle (season) apparent 0 end-member TA and *in situ* catchment TA values were computed from the Y-intercept of TA versus S cross-

correlations (Fig. 4a) and *in situ* TA measurements carried out at the same time over the Arcachon lagoon watershed watercourses (Polsenaere et al. 2012b) calculated here as discharge-weighted TA means, respectively (Fig. 4b). Apparent 0 end-member TA values were generally higher than *in situ* catchment values except during the end of summer and autumn period (September and November 2008, Fig. 4b).

Water pCO_2 averaged 496 ± 36 ppmv over the sampling years and were always oversaturated whatever the season and period of the day and tide, with regards to the atmospheric equilibrium of 390 ppmv (Figs. 2, 3, 5, Table 1). Mean values ranged from 461 ± 14 ppmv in July 2008 to 530 ± 39 ppmv in September 2009 (minimum and maximum values in summer/autumn) with in general (except between November and July 2008 and between April and September 2009) only significant differences between seasons (Kruskal-Wallis test, $p<0.05$) though lower than those observed at the diurnal/tidal scale (Table 1, Figs. 2, 3, 5).

Seasonal variations in *in situ* measured temperature, pCO_2 values and in temperature ($TpCO_2$, $tpCO_2$) versus non-temperature ($NpCO_2$) effects on pCO_2 are presented in Figure 2. During 2008, pCO_2 values showed weak seasonal variations increasing from April 2008 (474 ± 14 ppmv) to September 2008 (515 ± 36 ppmv) before decreasing towards November 2008 (463 ppmv). In 2009, pCO_2 increased from January to April (525 ± 14 ppmv) before decreasing towards June (490 ± 27 ppmv) and increasing again to September (530 ± 39 ppmv, Table 1, Fig. 2) as in 2008. In 2008, $NpCO_2$ values showed larger seasonal variations first decreasing from April to July (557 ± 22 and 381 ± 16 ppmv respectively), and then increasing towards November (583 ± 27 ppmv). To the contrary in 2009, a decrease was first observed from January (698 ± 16 ppmv) to June 2009 (417 ± 24 ppmv) before increasing towards September (463± 37 ppmv). In 2008 and 2009 respectively, $TpCO_2$ followed exactly the opposite patterns. Peak-to-peak seasonal amplitudes in *in situ* temperature and pCO_2 values were 9.9 °C and 52 ppmv in 2008 and 12.6 °C and 50 ppmv in 2009 (Fig. 2, Table 1).

3.1.2. At the diurnal/tidal time scales

Significant variations in inorganic carbon and associated parameters occurred at the diurnal/tidal scales (Table 1, Figs. 2, 3, 5). Water heights ranged from 0.4 m (July 2008 and June 2009) at low tide to 4.5 m (July 2008, January and June 2009) at high tide (Fig. 3). The largest salinity variation occurred during winter and spring with for instance 5.2 and 6.7 salinity unit difference between low and high tides in January and April 2009 respectively. During these seasons, at low tide, the lowest salinity values of 20.4 and 24.8 respectively were observed. To the contrary, during summer and autumn seasons, salinity values were higher (minimum values 30.2 at low tide in July 2008 and June 2009) and varied by less than 2.4 units throughout the tidal cycle (Table 1, Figs. 3, 5). Water temperature variations at the tidal/diurnal scales were small and ranged from 1.4/1.3 °C in September 2008/2009 to 3.3 °C in June 2009 (Table 1, Figs. 3, 5).

With regards to inorganic carbon parameters, DIC and TA concentrations showed weak diurnal/tidal variations with significant differences between high and low tides except in September 2008 (ranges of 0.078 mmol $kg^{-1}$for TA and 0.069 mmol kg^{-1} for DIC) and in June 2009 where lower values were measured during low tide periods, concomitant to lower salinities. δ^{13}C-DIC values were significantly higher during high tide in July 2008 and June 2009 (ranges: -1.7 to 0.2 ‰ and -0.4 to 0.2 ‰, respectively) (Table 1, Fig. 3).

Water pCO_2 tidal/diurnal variations ranged between 50 ppmv in winter and spring (51 and 54 ppmv in January 2009 and April 2008 respectively) to 150-200 ppmv in summer and autumn (148 and 192 ppmv in September 2009 and 2008) (Figs. 2, 3, 5). Whatever the season and hour, water pCO_2 values were always oversaturated compared to the atmospheric value of 390 ppm; at minimum over all tidal/diurnal cycles, pCO_2 value dropped to 405 ppmv in September 2008) (Table 1, Figs. 2, 3, 5). Some significant pCO_2 variations also occurred in the creek between nighttime and daytime and between the emersion and the immersion of the tidal flat (LT_D,

LT_N, HT_D and HT_N periods, see Fig. 5 caption and M&M section) (Non-parametric Mann-Whitney test, $p<0.05$) (Figs. 3 and 5, Table 1). In winter-spring (April 2008, November 2008, January 2009 and April 2009), during daytime pCO_2 were significantly higher and daytime salinity were lower than at night. To the contrary, in summer-autumn (July 2008, September 2008/09 and June 2009), daytime pCO_2 values were significantly lower than nighttime pCO_2 and salinity were higher at night. During the eight cycles, pCO_2 values at low tide were significantly higher than values at high tide (salinity values at low tide were also below high tide values) (Figs. 2, 3, 5, Table 1).

A correlation analysis showed significant negative correlations between water pCO_2 and salinity (or water height) values (i.e. Spearman coefficients pCO_2 versus salinity of -0.69 and -0.92, $p<0.01$ in July 2008 and September 2009 respectively), except in September and November 2008 (Fig. 3). pCO_2 values were also negatively correlated to δ^{13}C-DIC values in July 2008 and over all 2019 cycles (R: -0.63, -0.72 and -0.58 in July 2008, January and June 2009 respectively, $p<0.01$). TA concentrations appeared to be always significantly and positively correlated to salinity (or water height) (R: 0.93 and 0.80, $p<0.01$ in September 2008 and April 2009 for instance) and to DIC concentrations (Figs. 2, 3). δ^{13}C-DIC values were significantly and positively correlated to salinity and water height (H) values in July 2008 and over all 2019 cycles (R: 0.45, 0.70 in July 2008 and April 2009 respectively, $p<0.01$), to TA values in September 2008 and over all cycles in 2019 (R: 0.46, 0.59 in September 2008 and 2009 respectively, $p<0.01$) and to DIC concentrations over all cycles in 2009 (R: 0.61 and 0.76 in April and June 2009 respectively) (Fig. 4).

3.2. Gas transfer velocities and atmospheric CO_2 fluxes from the Arcachon lagoon waters

Wind speeds (U_{10}) ranged between 2.41 ± 1.05 and 7.74 ± 1.77 m s^{-1} in September and November 2008 respectively with significant differences noticed between September 2008 - January 2009 (minimum values) and July - November 2008 - September 2009 (maximum

values) (Kruskal-Wallis and Dunn's post-test, $p < 0.01$, Table 2). k_{600} values were in average estimated at 8.54 ± 6.75, 17.29 ± 15.76 and 17.00 ± 6.23 cm h^{-1} according to W92, RC01 and A09 equations respectively (see Material and Methods, Table 2). Minimum mean values occurred in September 2008 - January 2009 (1.82 ± 1.25, 4.4 ± 1.36 and 9.58 ± 3.3 cm h^{-1} in January 2009 with the three methods respectively, Table 2) whereas the highest values were reached in November 2008 - September 2009 (19.37 ± 8.37, 33.33 ± 19.51 and 28.38 ± 6.12 cm h^{-1} in November 2008 with the three methods respectively, Table 2). In April 2008 and September 2009 at high tide, k_{600} (and U_{10}) values were also found significantly different between day (higher values) and night (lower values) periods (Mann-Whitney test, $p < 0.05$) whatever used methods (Table 2).

Mean water-air CO_2 fluxes were estimated at 0.27 ± 0.22, 0.56 ± 0.54 and 0.55 ± 0.22 mmol m^{-2} h^{-1} according to W92, RC01 and A09 equations respectively (Table 2). Minimum mean values were observed in January 2009 (0.06 ± 0.04, 0.14 ± 0.06 and 0.29 ± 0.13 mmol m^{-2} h^{-1} with the three methods respectively) whereas the highest values were reached in September 2009 (0.62 ± 0.66, 1.67 ± 2.36 and 0.82 ± 0.47 mmol m^{-2} h^{-1} with the three methods respectively, Table 2). In April 2008 and September 2009, water-air CO_2 flux values were also found significantly different between day (higher values) and night (lower values) periods (Mann-Whitney test, $p < 0.05$) as it was the case for k_{600} and U_{10} values whatever used methods (Table 2). Water-air fluxes estimated from A09 equation were significantly higher than values estimated from W92 (and RC01) equations (Kruskal-Wallis and Dunn's post-test, $p < 0.01$) except in November 2008 - April 2009 - September 2009 where no significant difference was observed between methods.

In July 2008, an atmospheric EC mast was deployed in the Arcachon lagoon simultaneously and close (at 1.8 km) to the 24 hours cycle location (Fig. 1, Table 2; Polsenaere et al. 2012a). During the whole tidal cycle in July 2008, EC fluxes averaged 0.45 ± 7.71 mmol m^{-2} h^{-1} and

ranged from -17.98 to 43.19 mmol m^{-2} h^{-1}. EC water-air CO_2 fluxes during the immersion were on average -1.39 ± 2.67 mmol m^{-2} h^{-1} and ranged from -12.38 to 2.10 mmol m^{-2} h^{-1} with significantly lower values during daytime period (Mann-Whitney test, $p < 0.05$). Significant differences were computed between direct water-air CO_2 fluxes measured during the immersion at the EC site and calculated CO_2 fluxes from pCO_2 records at the channel site according to RC01 - A09 equations (Kruskal-Wallis and Dunn's post-test, $p < 0.01$; Table 2).

4. Discussion

4.1. Seasonal compensation of thermal and non-thermal effects on water pCO_2

In the Arcachon lagoon, seasonal variations in water inorganic carbon parameters and especially pCO_2 were relatively weak and on the lower range for waters influenced by an intertidal ecosystem when compared to other coastal ecosystems worldwide (Borges et al. 2005; Table 3). We observed a maximal pCO_2 variation of 196 ppmv between the lowest and the highest values measured during each 12- or 24-hour cycles and the maximum pCO_2 (averaged over each 24-hour cycle) amplitude barely reached 70 ppmv.

At the seasonal scale over coastal bays, thermal but also non-thermal effects can significantly influence water pCO_2 variations. In the studied lagoon, we observed that, seasonally, biological effects that consisted in more heterotrophy in winter and more autotrophy in summer, was offset by the thermal effect induced by the variation of water temperature (from 8.9 to 22.2 °C) resulting in relatively constant pCO_2 values throughout the year. Furthermore, other non-thermal effects were induced by mixing of freshwater in the lagoon, particularly in January 2009 when salinity decreased down to 20.4 (Table 1, Figs. 3, 4). River waters discharging in the lagoon are yearly oversaturated in CO_2 (Polsenaere et al. 2012b) and their positive influence on pCO_2 values was supposed to be maximal in January 2009 (Table 1, Fig. 3). Overall, thermal and non-thermal components of pCO_2 strongly varied seasonally, almost compensating each

other. For instance, the six months $\Delta TpCO_2$ offset (260 ppmv) observed from July 2008 to January 2009 ($TpCO_2$ from 601 to 341 ppmv) concomitantly to the 13.3 °C water temperature decrease (from 22.2 to 8.9 °C) barely compensated non-thermal effects on water pCO_2 that occurred during that six-month period ($\Delta NpCO_2$ = 317 ppmv, from 381 to 698 ppmv) (Fig. 2). In spring and summer, more autotrophic metabolism by all benthic and planktonic primary producers of the lagoon is favored and less remineralization occurs resulting in the lowest $NpCO_2$ values, while the effect of autotrophy on pCO_2 is offset by water heating. Phytoplankton blooms occur in the lagoon especially from the spring season that shows the highest primary production rates (between 231.4 and 496.6 mg C m^{-3} d^{-1} in 2003, Glé et al. 2008). Influxes of CO_2 in spring and early autumn were measured on the flat by the EC station (Polsenaere et al. 2012a). *Zostera* seagrass meadows also contribute significantly to the total primary production of the Bay (Plus et al. 2015; Polsenaere et al. 2012a; Ribaudo et al. 2017) and then may influence pCO_2 dynamics as observed elsewhere in the eastern shore of Virginia by Berg et al. (2019). In summer in the lagoon, higher *Zostera* seagrass net primary production associated with lower heterotrophic respiration result in more autotrophic sediment metabolism; together with phytoplanktonic and immersed *Zostera* production and lower freshwater inputs to the lagoon explain the $NpCO_2$ drawdown from January to June 2009 (281, from 698 to 417 ppmv). However, in summer, *Zostera* primary production probably occurs using mostly CO_2 directly from the atmosphere during the emersion and even more if low tide is around midday (Polsenaere et al. 2012a). Thus, in the studied channel the direct influence of *Zostera* metabolism on water pCO_2 is probably modest. To the contrary from spring to summer-autumn 2009 periods, $NpCO_2$ values increased (46, from 417 to 463 ppmv) whereas primary production decreased. In autumn and winter contrarily to summer season, heterotrophy is favored because the seagrass biomass is recycled and decomposed in the sediments and the waters (Auby and Labourg 1996). The *Zostera* meadow decline feeds the lagoon sediments and waters with

organic matter, favoring heterotrophy which together with a lower planktonic primary production and also more freshwater inputs to the lagoon, contribute to the highest $NpCO_2$ values measured in November 2008 and January 2009 (Fig. 2). At the same time, this combination of all factors on water pCO_2 is compensated by water cooling and in consequence, a pCO_2 value seasonally constant at about 500 ppmv was measured in the lagoon. Other studies showed a more pronounced effect of either thermal or non-thermal variations on water pCO_2 at the seasonal scale as for instance Ribas-Ribas et al. (2011) that reported in the Bay of Cadiz during winter a dominant thermal control in comparison with non-thermal effects, or to the contrary, Bozec et al. (2011) who showed in the Bay of Brest, a stronger influence of non-thermal (biology) processes on seasonal pCO_2 dynamics (Table 3).

4.2. Seasonal carbonate chemistry and mixing patterns of freshwater and seawater DIC

Besides biological activity and its light-temperature controlled seasonal evolution, horizontal advection and exchanges between terrestrial-lagoon-oceanic waters producing different mixing patterns, strongly drives observed carbonate chemistry at the seasonal scale in the lagoon. Hydrodynamic forcing importance was shown in other tidal systems such as a freshwater or salty marshes where intense exchanges between marsh and coastal/estuarine waters occurred during hydrological floods (Neubauer and Anderson 2003, and references in Table 3). Intense exchanges of oceanic and continental waters occurred within the Arcachon lagoon as well through channels or over the tidal flat around high tide (Plus et al. 2009; Polsenaere et al. 2012a, b). A significant influence of freshwater discharge in the lagoon occurred in winter of the year 2009 with the lowest salinities (20.5-24.5) associated to the lowest TA concentrations (1.493-1.733 mmol kg^{-1}) measured through our tidal cycle sampling (Fig. 3e). These low values especially at low tide reflected the freshwater inputs to the lagoon from rivers draining the podzolized acidic catchment (Polsenaere et al. 2012b). Furthermore, in the lagoon, water

seasonal mean TA values were always above corresponding DIC concentrations (maximum hourly measured DIC values were below minimum TA values too) except in January and April 2009. It highlights the seawater influence at the sampled channel station in the middle position inside the lagoon where CO_3^{2-} provides the first line of buffering capacity as observed by Wang et al. (2016) in the Sage Lot Pond salt marsh system. The significant positive correlations between δ^{13}C-DIC values and salinity values, TA values and DIC concentrations over all 2019 cycles (Fig. 4a, c, d) supports the importance of alkalinity (CO_3^{2-}) among other DIC species and thus an overall seasonal DIC variation control through tidal forcing.

Comparing apparent 0 end-member TA and *in situ* catchment TA values at each cycle (season), we highlighted that alkalinity production occurred within the lagoon especially in April, July 2008 and September 2009 when 0 end-member TA values were at least two times higher than *in situ* catchment weighted mean TA values (Fig. 4b). The Arcachon flat constitutes an important stock of carbonates of about 120 Mt of several shellfish species represented at 95 % by *Crassostrea gigas* (Polsenaere et al. 2012a). From the end of the reproduction season (November) to the spat removing in spring, early development stages of bivalves are particularly sensitive to dissolution-induced mortalities as shown by Barros et al. (2013) through larval viability laboratory experiments on the Pacific oyster *Crassostrea gigas*. Thus, $CaCO_3$ dissolution could occur in wet mud sediments in presence of such shellfishes patchily distributed on the tidal flat. To the contrary, in late summer (September) and autumn (November) 2008, *in situ* catchment TA values were slightly higher than 0 end-member TA values supporting the possibility of calcification processes in the lagoon (Fig. 4b). Seagrass systems are recognized to be important site of high calcium carbonate ($CaCO_3$) cycling, both in terms of production and dissolution, such as *Posidonia oceanica* meadows where $CaCO_3$ precipitation can overwhelm sediment $CaCO_3$ dissolution particularly during net autotrophic

periods (Barron et al. 2006). In any cases, net TA production in the lagoon remains more important in comparison with calcification at the annual scale.

4.3. Processes controlling tidal and diurnal pCO_2 and DIC variations

4.3.1. Large tidal DIC variations through current advection

Over intertidal systems as Arcachon, horizontal advection can strongly control water pCO_2 and carbonate chemistry variations at the tidal scale too. Significant negative correlations between pCO_2 and salinity or water height occurred most of the time in each season (except in Sept. and Nov. 08) and for each tidal/diurnal periods. The fact that higher pCO_2 values associated to lower salinity and depth values at low tide (opposite pattern during high tide) were systematically measured irrespective of day or night status supports the significant tidal rhythm control on water pCO_2 in the lagoon. For example, during the June 2009 cycle, pCO_2 and TA values were significantly inversely correlated and respectively negatively and positively correlated to water height, salinity and δ^{13}C-DIC values. Significantly higher TA concentrations associated to higher δ^{13}C-DIC values (typical oceanic TA and δ^{13}C-DIC values) were also measured during high tide periods contrarily to pCO_2 values (Table 1, Fig. 3). These results clearly reflected tidal forcing on carbonate chemistry through ocean exchange with more buffered waters on one hand and riverine inputs with more acidic waters on the other hand. In the Arcachon lagoon, maximum pCO_2 values measured at low tide were well below those measured over other coastal systems as tidal flats nearby and small marsh-estuary or mangrove tidal creeks further (Table 3). A 24 hour-cycle performed in May 2006 (not shown) in a shallower creek close to the outlet of a small river North East in the back of the Arcachon lagoon showed the highest pCO_2 values (up to 1300 ppmv, salinity values close to 28) at mid-ebb when the tidal flat was still immersed compared to the low tide period, when the flat was emerged and the channel connected to the river, with associated decreased and lower pCO_2 and salinity values (close to 800 ppmv and

22-23, respectively, data not shown). Thus, these measurements suggest another associated process (i.e. tidal pumping, see next 4.3.2. discussion part) along with freshwater mixing that occur together in the Arcachon flat.

4.3.2. Tidal porewater pumping and associated water alkalinity production and pCO_2 variations

During tidal cycles conducted at the channel station, TA (or DIC) concentrations showed overall weak tidal variations (Fig. 3). Porewater pumping over tidal coastal vegetated ecosystems (seagrass meadows, salt marshes and mangroves) has been recognized as an important process in water DIC production (Neubauer and Anderson 2003; Wang et al. 2016; Borges et al. 2003; Maher et al. 2013). Indeed, high alkalinity values can be reached through aerobic respiration coupled to carbonate dissolution but also through organic matter anaerobic remineralization products, i.e. N_2 from net denitrification and reduced sulfur (pyrite burial) from net sulfate reduction (Hu and Cai 2011). In Arcachon, tidal pumping has been highlighted as a significant process controlling benthic phosphorus and iron cycles over seagrasses where below the rhizosphere, Fe(II) can be exposed to a reduced environment and precipitates as FeS and pyrite (Deborde et al. 2008b). De Wit (2008) showed the importance of sulfate-reducing bacteria in *Zostera* seagrass sediments at a tidal flat station very close to our 24-hour cycle station. Moreover, Heijs et al. (1999) showed at the same location that a substantial population of aerobic sulfide-oxidizing bacteria was also present, buffering free sulfide through chemical processes with iron leading to high FeS and pyrite concentrations in sediments. In particular, sulfide oxidation (depending on whether sulfide will be oxidized to sulfate or to sulfur) was estimated at 4694 x 10^3 or 1174 x 10^3 mol cm^{-3} day^{-1}, whereas previously measured sulfate reduction rates at the same station ranged from 150 to 1300 nmol cm^{-3} day^{-1}. These findings along with the quantitative apparent 0 end-member and *in situ* catchment TA value (Fig. 4b)

suggest a substantial TA production though tidal porewater pumping along the year. Its influence on TA (or DIC) production in the lagoon could not be clearly seen from our chosen site, which have high salinities and TA values, hiding the terrestrial influence and did not cover the 0 end-member. In any cases, in Arcachon, alkalinity production through tidal pumping is not so strong in comparison with other mentioned mangrove or saltmarsh systems. Maher et al. (2013) measured in a small tidal mangrove creek (Australia) during summer and winter a clear tidal trend for DIC as in the present study (highest and lowest values reached during low and high tides, respectively). However, a 0.736 mmol kg^{-1} DIC range (between 2.064 and 2.8 mmol kg^{-1}) was measured there when in the Arcachon channel we only measured a tidal DIC variation of 0.216 mmol kg^{-1} (April 2009) at maximum (0.116 mmol kg^{-1} in average over the whole study period). In the Sage Lot Pond tidal marsh, Wang et al. (2016) measured in Summer tidal TA variation ranges close to 0.4 mmol kg^{-1} respectively when at Arcachon a variation of 0.261 mmol kg^{-1} at maximum (0.133 mmol kg^{-1} in average) was seen. Similarly, according to tidal pCO_2 variations, smaller variations were measured in comparison to other salt marsh-estuary or mangrove creek systems, where stronger tidal pCO_2 variations were observed according to porewater mixing (Table 3).

4.3.3 Significant diurnal pCO_2 patterns linked to biological activity

In subtidal coastal ecosystems, pelagic and benthic biological activities can generate large diurnal water pCO_2 variations. Indeed, in comparison with Arcachon, similar and even higher diurnal pCO_2 ranges were measured in macrophyte meadows (Baltic Sea, Florida and Virginia) or in bay channels (Spain) (Table 3). However, in these subtidal ecosystems, tidal pumping was supposed to be minor; in the Arcachon lagoon, pCO_2 variations occur at the tidal scale through porewater pumping and water masses mixing, these latter being superposed on those occurring at the diurnal scale and linked to solar radiation and light availability.

During all sampled cycles, no significant pCO_2 versus Chl-*a* concentration relationships were computed and Chl-*a* concentrations never reached more than 1.9 µg L^{-1} in average (data not shown). Our successive tidal/diurnal cycle samplings in the central lagoon channel were apparently not able to fully catch these blooms especially in spring and summer. However, interesting diurnal pCO_2 patterns related to biological activity could be detected when comparing nighttime with daytime values for a same salinity range. For instance, in September 2008, at low tide in the channel for a salinity range values close to 33, lower water pCO_2 and higher temperature values were measured at daytime (400-525 ppmv, > 20 °C) than at nighttime (550-600 ppmv, close to 19 °C) (Fig. 5e, f). The same pattern was observed in June 2009 as well (Fig. 5m, n). Phytoplankton possibly with resuspended microphytobenthos communities in the channel then appeared to be active at that moment. Savelli et al. (2019) showed precisely that almost half (43 %) of MPB primary production can be resuspended annually over intertidal lagoons and the highest occurs in spring tide at the flood beginning due to high current velocities and low water heights. To the contrary, in April 2009 during flooding, water pCO_2 (500-560 ppmv) increased (while S increased and T decreased) whereas during ebbing, water pCO_2 (538-494 ppmv) decreased and was lower (while S decreased and T increased) (Fig. 5k, l). At that particular moment in the channel, organic matter produced by primary production could feed community respiration through incoming coastal waters during flooding. The significant negative correlation computed between pCO_2 and δ^{13}C-DIC values is consistent with an organic matter mineralization process that occurred in spring in the lagoon.

To assess the biological control on measured pCO_2 patterns in the studied channel, we statistically compared, when possible, night and day pCO_2 values averaged over the same salinity range (i.e. with no significant salinity value difference between day and night periods) according to tide phases for each cycle (Table 4). During flooding, daytime pCO_2 were significantly lower than those nighttime pCO_2 values and to the contrary, during ebbing phase,

daytime pCO_2 were significantly higher night time pCO_2 values. At the same time, significant variations in water temperature between day and night times for both flooding and ebbing periods occurred. Water temperature gradients exist and could influence diurnal pCO_2 variations. However, they cannot alone explain these variations at our sampling station since differences between the theoretical pCO_2 variations due to diel temperature differences and measured changes in water pCO_2 for the same salinity range are large (Table 4).

Overall, these reproductible patterns strongly support the control of pCO_2 by biological activity (primary production of phytoplankton, MPB and seagrasses). Koné et al. (2009) reported pCO_2-oversaturated waters in some lagoons of Ivory Coast (West Africa) behaving as macrotidal estuaries due to net ecosystem heterotrophy and riverine CO_2 rich water inputs. To the contrary pCO_2-undersaturated waters were found in the other lagoons showing permanent hyaline stratification leading to higher phytoplankton biomass. In other systems such as Tampa and Florida bays, pCO_2 diurnal variability was mostly influenced by biological processes such as photosynthesis/respiration of benthic communities and precipitation/dissolution of calcium carbonate respectively (Table 3). Interestingly and contrary to other studied salt marsh and mangrove systems (Table 3) where tidal pumping is predominant, water pCO_2 and DIC variations in the Arcachon lagoon seemed to result from the subtle combination of thermal, water column primary production, and tidal pumping effects along with thermodynamic mixing between seawater and freshwater.

4.4. High heterogeneity in water-air CO_2 fluxes over the Arcachon lagoon

4.4.1. Turbulence forcing control on water-air CO_2 flux temporal variability

The subsurface waters of the Arcachon lagoon remained always oversaturated and close to the atmospheric equilibrium at both seasonal and diurnal scales. Annual mean air-sea CO_2 fluxes were estimated at 0.27 ± 0.22, 0.56 ± 0.54 and 0.55 ± 0.22 mmol m^{-2} h^{-1} depending on the gas

transfer velocity-wind parameterizations. Water-air CO_2 flux values remained in the lower range of annual values reported for macrotidal estuaries (0.58-8.42 mmol m^{-2} h^{-1}) (Borges et al. 2005). Similar intertidal systems showed different values with more variations at both diurnal and seasonal scales (Table 3). In other subtidal and marine systems, fluctuations between CO_2 sink and source could also be measured over the year depending on seasons (Table 3).

In the Arcachon lagoon, wind speed influence on calculated air-sea CO_2 fluxes was significant and could be more important in determining the intensity of the flux, than the pCO_2 air-sea gradient itself. Despite significant pCO_2 variations generally noticed at seasonal and tidal/diurnal scales, only few significant air-sea CO_2 flux differences were observed (i.e. between November and September 2008 and between September 2008 and 2009), concomitantly to significant differences in U_{10} and K_{600} values (Table 2). Thus, air-sea CO_2 flux variability in the Arcachon lagoon at all temporal scales appears to be controlled by turbulence (K_{600}, physical forcing) rather than air-water pCO_2 gradients. This finding is the opposite of what it is generally observed over dynamic coastal bays at temperate and tropical latitudes characterized by higher diurnal/tidal water pCO_2 gradients (Table 3).

4.4.2. High heterogeneity in water-air CO_2 fluxes according to space and methodology

CO_2 fluxes were estimated at the water-air interface based on k_{600} parameterizations from Wanninkhof et al. (1992), Raymond and Cole (2001) and Abril et al. (2009). These parameterizations were obtained over oceanic and estuarine systems with different approaches, i.e. the bomb ^{14}C inventory in the ocean, non-intrusive tracer data and chamber measurements respectively. The Abril et al. (2009) relationship gave significantly higher flux values compared to the two others, potentially due to bottom current contributions from 2 to 20 cm s^{-1} according to seasons and associated hydrodynamic modelling estimations. In July of the year 2008, significant differences were computed between simultaneous direct EC fluxes and estimated

fluxes from gas transfer parameterizations (Table 2). No k_{600} calculations or flux data comparisons were attempted from these simultaneous EC flux and water pCO_2 measurements due to strong spatial heterogeneity in water bodies (separated from 1.8 km) highlighted in the present study and due to the strong variability in gas transfer velocity and CO_2 flux calculations according to methodologies too (Polsenaere et al. 2012a; Raymond and Cole 2001; Vachon et al. 2010).

Indeed, variability in water pCO_2 and air-sea CO_2 fluxes depends on site locations inside a same coastal ecosystem at the different temporal scales. The spring 2006 cycle carried out in the back of the Arcachon lagoon (4.3.1. discussion part) showed higher water pCO_2 tidal variations (680-1330 ppmv) and resulted in a higher CO_2 source to the atmosphere at this more terrestrial influenced location. These observations suggest that large differences in water pCO_2 and sea-air CO_2 fluxes could occur at smaller spatial scale due to specific processes and characteristics that exist at the sampled area. In the lagoon, benthic primary producers such as *Zostera noltei* seagrass meadows and resuspended microphytobenthic communities could influence in a different way carbon dynamics and air-sea fluxes at the channel station sampled here, compared to swallow waters above the tidal flat as revealed by EC measurements (Polsenaere et al. 2012a). Indeed, a CO_2 influx was detected during the emersion by the EC, but we never observed CO_2 undersaturated waters in the channel during the July 2008 cycle. Due to the strong influence of tidal advection on water pCO_2 in the intertidal lagoon, water masses sampled at the studied station were not the same as those caught in the EC footprint during in July 2008 (Tables 1 and 2, Polsenaere et al. 2012a). This could also explain the significant differences in air-sea CO_2 fluxes and associated gas transfer velocities we got from both methodologies, and methodological and logistical complexity to get concomitant water-air EC flux and equilibrator water pCO_2 values from the same water mass in the lagoon. Wang et al. (2018) over the Duplin River salt marsh-estuary (Georgia), though different from Arcachon due to the most of the time

emersion canopy (ecosystem-atmosphere flux there versus water-atmosphere flux based on water pCO_2 here) specifically suggested EC measurements of salt marsh net ecosystem exchange could underestimate net ecosystem production for not accounting for lateral DIC exchanges with tidal inundation.

Conclusions

Waters of the Arcachon lagoon represents a permanent weak CO_2 supersaturation characterized by a seasonal compensation of thermal and biological effects and carbonate chemistry and mixing patterns of freshwater and seawater DIC. At smaller time scales if large tidal DIC variations through current advection were observed, weak tidal porewater pumping and associated water alkalinity production and pCO_2 variations were noticed compared to other tidal creeks surrounded by mangrove or saltmarshes. Accurate water monitoring such as that carried out in this study permits high resolution analysis of the carbon signal; small but significant pCO_2 variations were seen at the diurnal scale (between 5 and 24 ppmv) linked to the light cycle apparently induced by planktonic and benthic productivity in the channel along to day versus night temperature gradients at flooding and ebbing periods. The temporal variability and the high heterogeneity in computed water-air CO_2 fluxes according to space (water masses) and methodology (EC, …) would require more integrated carbon fluxes and processes over tidal ecosystems as here for the Arcachon lagoon.

Acknowledgments

We would like to express our thanks to Francis Prince the Planula boat captain. This paper is a contribution to the PNEC (Programme National Environnement Côtier)-Littoral Atlantique and ANR PROTIDAL (Agence Nationale de la Recherche « Processus biogéochimiques transitoires de la zone intertidale ») projects.

Competing Interests

The authors declare no competing interests.

References

Abril, G., M. Commarieu, A. Sottolichio, P. Bretel, and F. Guérin. 2009. Turbidity limits gas exchange in a large macrotidal estuary. *Estuarine, Coastal and Shelf Science* 83: 342–348.

Abril, G., Deborde, J., Savoye, N., Mathieu, F., Moreira-Turcq, P., Artigas, F., Meziane, T., Takiyama, L. R., de Souza, M. S., Seyler, P. 2013. Export of ^{13}C-depleted dissolved inorganic carbon from a tidal forest bordering the Amazon estuary. *Estuarine, Coastal and Shelf Science*, 129: 23-27.

Amanieu, M. 1967. Recherches écologiques sur la faune des plages abritées et des étangs saumâtres de la région d'Arcachon. *PhD Thesis, Université Bordeaux 1*, pp. 234.

Amorocho, J. and J.J. DeVries. 1980. A new evalution of the wind stress coefficient over water surfaces. *Journal of Geophysical Research* 85: 433–442.

Auby, I., F. Manaud, D. Maurer, and G. Trut. 1994. Étude de la prolifération des algues vertes dans le bassin d'Arcachon. *Report Prepared by IFREMER, Arcachon, France, for CEMAGREF-SSA-SABARC*, pp. 1–163.

Auby, I. and P.J. Labourg. 1996. Seasonal dynamics of *Zostera noltii* Hornem. in Bay of Arcachon (France). *Journal of Sea Research* 35: 269–277.

Barron, C., C. M. Duarte, M. Frankignoulle, and A.V. Borges. 2006. Organic carbon metabolism and carbonate dynamics in a Mediterranean seagrass (*Posidonia oceanica*) meadow. *Estuaries and Coasts* 29: 417–426.

Barros, P., P. Sobral, P. Range, L. Chícharo, and D. Matias. 2013. Effects of sea-water acidification on fertilization and larval development of the oyster *Crassostrea gigas*. *Journal of Experimental Marine Biology and Ecology* 440: 200–206. https://doi.org/10.1016/j.jembe.2012.12.014.

Bauer, J.E., W.-J. Cai, P.A. Raymond, T.S. Bianchi, C.S. Hopkinson, and P.A.G. Regnier. 2013. The changing carbon cycle of the coastal ocean. *Nature* 504 (7478): 61–70.

Berg, P., M.L. Delgard, P. Polsenaere, K.J. McGlathery, S.C. Doney S.C., and A.C. Berger. 2019. Dynamics of benthic metabolism, O_2, and pCO_2 in a temperate seagrass meadow. *Limnology and Oceanography* 64: 2586–2604.

Borges, A.V. and M. Frankignoulle. 1999. Daily and seasonal variations of the partial pressure of CO_2 in surface seawater along Belgian and southern Dutch coastal areas. *Journal of Marine Systems* 19 (4): 251–266.

Borges, A. V., S. Djenidi, G. Lacroix, J. Théate, B. Delille, and M. Frankignoulle. 2003. Atmospheric CO_2 flux from mangrove surrounding waters. *Geophysical Research Letters* 30(11), 1558. https://doi.org/10.1029/2003GL017143.

Borges, A. V., B. Delille, and M. Frankignoulle. 2005. Budgeting sinks and sources of CO_2 in the coastal ocean: diversity of ecosystems counts. *Geophysical Research Letters* 32: LI4601. https://doi:10.1029/2005GL023053.

Borges, A.V. and G. Abril. 2011. Carbon dioxide and methane dynamics in estuaries. In *Treatise on estuarine and coastal science*, ed. E. Wolanski and D.S. McLusky 5: 119–161.

Bouillon, S., Middelburg, J.J., Dehairs, F., Borges, A.V., Abril, G., Flindt, M.R., Ulomi, S., Kristensen, E. 2007. Importance of intertidal sediment processes and porewater exchange on the water column biogeochemistry in a pristine mangrove creek (Ras Dege, Tanzania). *Biogeosciences 4* (3): 311–322.

Bozec, Y., L. Merlivat, A.-C. Baudoux, L. Beaumont, S. Blain, E. Bucciarelli, T. Danguy, E. Grossteffan, A. Guillot, and J. Guillou. 2011. Diurnal to inter-annual dynamics of pCO_2 recorded by a CARIOCA sensor in a temperate coastal ecosystem (2003–2009). *Marine Chemistry* 126: 13–26.

Burgos, M., T. Ortega, and J. Forja. 2018. Carbon Dioxide and Methane Dynamics in Three Coastal Systems of Cadiz Bay (SW Spain). *Estuaries and Coasts* 41: 1069–1088. https://doi.org/10.1007/s12237-017-0330-2.

Cai, W.J., L.R. Pomeroy, M.A. Moran, and Y. Wang. 1999. Oxygen and carbon dioxide mass balance for the estuarine-intertidal marsh complex of five rivers in the southeastern US. *Limnology and Oceanography* 44: 639–649.

Cai, W.-J. 2011. Estuarine and coastal ocean carbon paradox: CO_2 sinks or sites of terrestrial carbon incineration? *Annual Review of Marine Science* 3 (1): 123–145.

Canton, M, P. Anschutz, A. Coynel, P. Polsenaere, I. Auby, and D. Poirier. 2012. Nutrient export to an Eastern Atlantic coastal zone: first modeling and nitrogen mass balance. *Biogeochemistry* 107: 361–377.

Caumette, P., J. Castel, and Herbert R. 1996. Coastal Lagoon Eutrophication and ANaerobic Processes (C.L.E.AN.): Nitrogen and Sulfur Cycles and Population Dynamics in Coastal Lagoons. *A Research Programme of the Environment Programme of the EC (DG XII)*. https://doi.org/10.1007/978-94-009-1744-6.

Chen, C.-T.A., Huang, T.-H., Chen, Y.-C., Bai, Y., He, X., Kang, Y. 2013. Air–sea exchanges of CO_2 in the world's coastal seas. *Biogeosciences* 10, 6509–6544. https://doi.org/10.5194/bg-10-6509-2013.

Cognat, M., F. Ganthy, I. Auby, F. Barraquand, L. Rigouin, and A. Sottolichio, 2018. Environmental factors controlling biomass development of seagrass meadows of

Zostera noltei after a drastic decline (Arcachon Bay, France). *Journal Of Sea Research* 140: 87–104.

Coignot, E., P. Polsenaere, P. Soletchnik, O. Le Moine, P. Souchu, E. Joyeux, Y. Le Roy, J.-P. Guéret, L. Froud, R. Gallais, E. Chourré, and L.Chaigneau. 2020. Variabilité spatio-temporelle des nutriments et du carbone et flux associés le long d'un continuum terrestre-aquatique tempéré (Marais poitevin – Baie de l'Aiguillon – Pertuis Breton). Rapport final (suivi 2017-2018) - Projet Aiguillon (2016-2020). 111pp. https://archimer.ifremer.fr/doc/00618/73003/

Cole, J.J., Y.T. Prairie, N.F. Caraco, W.H. Mcdowell, L.J. Tranvik, R.G. Striegl, C.M. Duarte, P. Kortelainen, J.A. Downing, J. Middleburg, and J. Melack. 2007. Plumbing the global carbon cycle: integrating inland waters into the terrestrial carbon budget. *Ecosystems* 10: 171–184.

Cotovicz, L.C., B.A. Knoppers, N. Brandini, S.J. Costa Santos, and G. Abril. 2015. A large CO_2 sink enhanced by eutrophication in a tropical coastal embayment (Guanabara Bay, Rio de Janeiro, Brazil). *Biogeosciences* 12: 6125–6146. https://doi.org/10.5194/bg-12-6125-2015.

Cotovicz, L.C., B.G.Libardoni, N.Brandini, B.A. Knoppers and G. Abril. 2016. Comparações entre medições em tempo real da pCO_2 aquática com estimativas indiretas em dois estuários tropicais contrastantes: o estuário eutrofizado da baía de Guanabara (RJ) e o estuário oligotrofico do rio São Francisco (AL). *Química Nova*. 39: 1206–1214. https://doi.org/10.21577/0100-4042.20160145.

Dai, M., Z. Lu, W. Zhai, B. Chen, Z. Cao, K. Zhou, W. J. Cai, and C. T. A. Chen. 2009. Diurnal variations of surface seawater pCO_2 in contrasting coastal environments. *Limnology and Oceanography* 54: 735–745.

Deborde, J., P. Anschutz, I. Auby, C. Glé, M.V. Commarieu, D. Maurer, P. Lecroart, G. Abril. 2008a. Role of the tidal pumping on nutrient cycling in a temperate lagoon (Arcachon Bay, France). *Marine Chemistry* 109: 98–114.

Deborde J., G. Abril, A. Mouret, D. Jezequel, G. Thouzeau, J. Clavier, G. Bachelet, P. Anschutz. 2008b. Impacts of seasonal dynamics impact of a *Zostera noltii* meadow on phosphorus and iron cycles in a tidal mudflat (Arcachon Bay, France), *Marine Ecology Progress Series* 355, 59–71.

Delgard, M. L., B. Deflandre, J. Deborde, M. Richard, C. Charbonnier, and P. Anschutz. 2013. Changes in Nutrient Biogeochemistry in Response to the Regression of *Zostera noltii* Meadows in the Arcachon Bay (France). *Aquatic Geochemistry* 19: 241–259. doi:10.1007/s10498-013-9192-9

Delille, B, AV Borges, and D. Delille. 2009. Influence of giant kelp beds (*Macrocystis pyrifera*) on diel cycles of pCO_2 and DIC in the sub-Antarctic coastal area. *Estuarine Coastal and Shelf Science* 81: 114–122.

De Wit, R. 2008. Microbial diversity in the Bassin d'Arcachon coastal lagoon (SW France). *Hydrobiologia* 611: 5–15. https://doi.org/10.1007/s10750-008-9461-6.

Dickson, A.G. and F.J. Millero. 1987. A comparison of the equilibrium constants for the dissociation of carbonic acid in seawater media. *Deep-Sea Research* 34: 1733–1743.

Dickson, A.G. 1990. Standard potential of the reaction: AgCl(s) + 1⁄2H2(g) = Ag(s) + HCl(aq), and the standard acidity constant of the ion HSO_4^- in synthetic sea water from 273.15 to 318.15 K. *Journal of Chemical Thermodynamics* 22: 113–127.

Fauvelle, V., A. Belles, H. Budzinski, N. Mazzella, and M. Plus . 2018. Simulated conservative tracer as a proxy for S-metolachlor concentration predictions compared to POCIS measurements in Arcachon Bay. *Marine Pollution Bulletin* 133: 423–427. https://doi.org/10.1016/j.marpolbul.2018.06.005.

Frankignoulle, M., I. Bourge, C. Canon, and P. Dauby. 1996. Distribution of surface seawater partial CO_2 pressure in the English Channel and in the Southern Bight of the North Sea. *Continental Shelf Research* 16: 381–395.

Frankignoulle, M., G. Abril, A.V. Borges I. Bourge, C. Canon, B. Delille, E. Libert, and J.M. Théate. 1998. Carbon dioxide emission from European estuaries. *Science* 282: 434–436.

Frankignoulle, M, A.V. Borges, and R. Biondo. 2001. A new design of equilibrator to monitor carbon dioxide in highly dynamic and turbid environments. *Water Research* 35: 344–1347.

Ganthy, F., A. Sottolichio, R. Verney. 2013. Seasonal modification of tidal flat sediment dynamics by seagrass meadows of Zostera noltii (Bassin d'Arcachon, France). *Journal Of Marine Systems* 109: 233–240. https://doi.org/10.1016/j.jmarsys.2011.11.027.

Gattuso, J.-P., M. Frankignoulle, and R. Wollast. 1998. Carbon and carbonate metabolism in coastal aquatic systems. *Annual Review Ecology Systematics* 29, 405–433.

Gazeau, F., V.S. Smith, B. Gentili, M. Frankignulle, and J.P. Gattuso. 2004. The European coastal zone: characterization and first assessment of ecosystem metabolism, *Estuarine, Coastal and Shelf Science* 60: 673–694.

Gillikin, D.P. and S. Bouillon. 2007. Determination of $\delta^{18}O$ of water and $\delta^{13}C$ of dissolved inorganic carbon using a simple modification of an elemental analyzer—isotope ratio mass spectrometer EA-IRMS: an evaluation. *Rapid Communication in Mass Spectrometry* 21: 1475–1478

Glé, C., Y. Del Amo, B. Sautour, P. Laborde, and P. Chardy. 2008. Variability of nutrients and phytoplankton primary production in a shallow macrotidal coastal ecosystem (Arcachon Bay, France), *Estuarine, Coastal and Shelf Science* 76 (3): 642–656.

Gran, G. 1952. Determination of the equivalence point in potentiometric titrations. Part II. *Analyst* 77: 661–671.

Heijs, S.K., H.M. Jonkers, H. van Gemerden, B.E.M. Schaub, and L.J. Stal. 1999. The Buffering Capacity Towards Free Sulfide in Sediments of a Coastal Lagoon (Bassin d'Arcachon, France) the Relative Importance of Chemical and Biological Processes. *Estuarine, Coastal and Shelf Science* 49 (1): 21–35. https://doi.org/10.1006/ecss.1999.0482.

Hu, X., and W.-J. Cai. 2011. An assessment of ocean margin anaerobic processes on oceanic alkalinity budget. *Global Biogeochemical Cycles* 25: GB3003. https://doi.org/10.1029/2010GB003859.

Jähne, B., K.O. Münnich, R. Bösinger, A. Dutzi, W. Huber, and P. Libner. 1987. On the parameters influencing air-water gas exchange. *Journal of Geophysical Research* 92*:* 1937-1949.

Kjerfve, B. 1985. Comparative oceanography of coastal lagoons. *In Estuarine variability, ed. D.A. Wolfe, New York Academic*, 63–81.

Koné, Y.J., G. Abril, K.N. Kouadio, B. Delille, and A.V. Borges. 2009. Seasonal variability of carbon dioxide in the rivers and lagoons of Ivory Coast (West Africa). *Estuaries and Coasts* 32: 246–260.

Laruelle, G. G, H. H. Durr, C. P. Slomp, and A. V. Borges. 2010. Evaluation of sinks and sources of CO_2 in the global coastal ocean using a spatially-explicit typology of estuaries and continental shelves. *Geophysical Research Letters* 37, L15607. https://doi.org/10.1029/2010GL043691.

Lazure, P., and F. Dumas. 2008. An external-internal mode coupling for a 3D hydrodynamical model for applications at regional scale (MARS). *Advances in water Resources* 31: 233–250. http://doi.org/10.1016/j.advwatres.2007.06.010.

Lee, K., T.W. Kim, R.H. Byrne, F. J. Millero, R. A. Feely, and Y.M. Liu. 2010. The universal ratio of boron to chlorinity for the North Pacific and North Atlantic oceans. *Geochimica et Cosmochimica Acta* 74: 1801–1811.

Lewis, E. and D. Wallace. 1998. Program developed for CO_2 system calculations. *Carbon dioxide information analysis center. Oak Ridge National Laboratory*.

Maher, D.T., I.R., Santos, L. Golsby-Smith, J. Gleeson, and B.D. Eyre. 2013. Groundwater-derived dissolved inorganic and organic carbon exports from a mangrove tidal creek: The missing mangrove carbon sink? *Limnology and Oceanography* 58: 1801–1811. https://doi.org/10.4319/lo.2013.58.2.0475.

Mantoura, R. F. C., J. M. Martin, and R. Wollast. 1991. Ocean margin processes. *In Global Change, Chichester, UK: Wiley & Sons*, pp. 469.

Mehrbach C, C.H. Culberson, J.E. Hawley, and R.N. Pytkowicz. 1973. Measurement of the apparent dissociation constants of carbonic acid in seawater at atmospheric pressure. *Limnology and Oceanography* 18: 897–907.

Migné, A., D. Davoult, N. Spilmont, V. Ouisse, and G. Boucher. 2016. Spatial and temporal variability of CO_2 fluxes at the sediment–air interface in a tidal flat of a temperate lagoon (Arcachon Bay, France). *Journal of Sea Research*, 109: 13-19. https://doi.org/10.1016/j.seares.2016.01.003.

Miyajima, T., Y. Yamada, Y.T. Hanba, K. Yoshii, T. Koitabashi, and E. Wada. 1995. Determining the stable isotope ratio of total dissolved inorganic carbon in lake water by GC/C/IRMS. *Limnology and Oceanography* 40: 994–1000.

Mook W. G., Koopmans M., Carter A. F., and Keeling C. D. 1983. Seasonal, latitudinal, and secular variations in the abundance and isotopic ratios of atmospheric carbon dioxide. 1. Results from land stations. *Journal of Geophysical Research* 88: 10915–10933.

Neubauer, S. C. and I. C. Anderson. 2003. Transport of dissolved inorganic carbon from a tidal freshwater marsh to the York River estuary. *Limnology and Oceanography* 48: 299–307. https://doi.org/10.4319/lo.2003.48.1.0299.

Parker S. R., Poulson S. R., Gammons C. H., and Degrandpre M. D. 2005. Biogeochemical controls on diel cycling of stable isotopes of dissolved O_2 and dissolved inorganic carbon in the Big Hole River, Montana. *Environmental Science Technology* 39: 7134–7140.

Pernetta, J.C. and J.D. Milliman. 1995. Land-Ocean interactions in the coastal zone. *Implementation plan, IGPB Rep.* 33: 1–215.

Plus, M., F. Dumas, J-Y. Stanisière, and D. Maurer. 2009. Hydrodynamic characterization of the Arcachon Bay, using model-derived descriptors. *Continental Shelf Research* 29(8): 1008-1013. https://doi.org/10.1016/j.csr.2008.12.016.

Plus, M., S. Dalloyau, G. Trut, I. Auby, X. de Montaudouin, E. Emery, C. Noel, and C. Viala 2010. Long-term evolution (1988–2008) of *Zostera* spp. Meadows in Arcachon bay (Bay of Biscay). *Estuarine, Coastal and Shelf Science* 87: 357–366.

Plus, M., I. Auby, D. Maurer, G. Trut, Y. Del Amo, F. Dumas, B. Thouvenin. 2015. Phytoplankton versus macrophyte contribution to primary production and biogeochemical cycles of a coastal mesotidal system. A modelling approach. *Estuarine Coastal and Shelf Science* 165: 52–60.

Polsenaere P., E. Lamaud, J.-M. Bonnefond, V. Lafon, P. Bretel, B. Delille, J. Deborde, D. Loustau, and G. Abril. 2012a. Spatial and temporal CO_2 exchanges measured by Eddy Covariance over a temperate intertidal flat and their relationships to net ecosystem production. *Biogeosciences* 9: 249-268.

Polsenaere, P. and G. Abril. 2012. Modelling CO_2 degassing from small acidic rivers using water pCO_2, DIC and δ^{13}C-DIC data. *Geochimica et Cosmochimica Acta* 91: 220-239.

Polsenaere P., N. Savoye H. Etcheber M. Canton D. Poirier, S. Bouillon and G. Abril. 2012b. Export and degassing of terrestrial carbon through watercourses draining a temperate podzolized catchment. *Aquatic Sciences*. https://doi.org/10.1007/s00027-012-0275-2.

Polsenaere P., R. Lannuzel, S. Guesdon, O. Le Moine, and P. Soletchnik. 2018. Variabilité spatio-temporelle des nutriments et du carbone et flux associés le long d'un continuum terrestre-aquatique tempéré (Marais poitevin - Baie de l'Aiguillon - Pertuis Breton). PROJET AIGUILLON (2016-2020). Rapport scientifique. 85 pp. *https://archimer.ifremer.fr/doc/00461/57284/*

Raymond, P. A. and J. J. Cole. 2001. Gas exchange in rivers and estuaries: choosing a gas transfer velocity. *Estuaries* 24: 312–317.

Ribas-Ribas, M., A. Gómez-Parra, and J.M. Forja. 2011. Air–sea CO_2 fluxes in the north-eastern shelf of the Gulf of Cádiz (southwest Iberian Peninsula). *Marine Chemistry* 123: 56–66. https://doi.org/10.1016/j.marchem.2010.09.005.

Ribas-Ribas, M., E. Anfuso, A. Gómez-Parra, and J.M. Forja. 2013. Tidal and seasonal carbon and nutrient dynamics of the Guadalquivir estuary and the Bay of Cádiz (SW Iberian Peninsula). *Biogeosciences* 10: 4481–4491.

Ribaudo C., V. Bertrin G. Jan, P. Anschutz, and G. Abril. 2017. Benthic production, respiration, and methane oxydation in *Lobelia dormanna* lawns. *Hydrobiologia* 784: 21–34. https://doi.org/10.1007/s10750-016-2848-x.

Rigaud S., B. Deflandre, O. Maire, G. Bernard, and P. Anschutz. 2018. Transient biogeochemistry in intertidal sediments: new insights from tidal pools in *Zostera noltei* meadows of Arcachon Bay (France). *Marine Chemistry* 200: 1–13. https://doi.org/10.1016/j.marchem.2018.02.002.

Rimmelin, P., J.C. Dumon, E. Maneux, and A. Gonçalves. 1998. Study of annual and seasonal dissolved inorganic nitrogen inputs into the Arcachon Lagoon, Atlantic Coast (France). *Estuarine Coastal Shelf Science* 47(5): 649–659.

Saderne, V., P. Fietzek, and P.M.J., Herman. 2013. Extreme Variations of pCO_2 and pH in a Macrophyte Meadow of the Baltic Sea in Summer: Evidence of the Effect of Photosynthesis and Local Upwelling. *PLoS One* 8: e62689.

Savelli, R., X. Bertin, F. Orvain, P. Gernez, A. Dale, T. Coulombier, P. Pineau, N. Lachaussée, P. Polsenaere C. Dupuy, and V. le Fouest. 2019. Impact of chronic and massive resuspension mechanisms on the microphytobenthos dynamics in a temperate intertidal mudflat. *Journal of Geophysical Research: Biogeosciences 124*. https://doi.org/10. 1029/2019JG005369.

Takahashi, T., S.C. Sutherland, C. Sweeney, A. Poisson, N. Metzl, B. Tilbrook, N. Bates, et al. 2002. Global sea–air CO_2 flux based on climatological surface ocean pCO_2, and seasonal biological and temperature effects. *Deep Sea Research Part II*: Topical Studies in Oceanography 49: 1601–1622. https://doi.org/10.1016/S0967- 0645(02)00003-6.

Ternon Q., P. Polsenaere, V. Le Fouest, J.-B. Favier, O. Philippine, J.-M. Chabirand, J. Grizon, and C. Dupuy. 2018. Étude des pressions partielles et flux de CO_2 au sein de la Communauté d'Agglomération de La Rochelle, rapport scientifique. pp. 32.

Vachon, D., Y. T. Prairie, and J. J. Cole. 2010. The relationship between near-surface turbulence and gas transfer velocity in freshwater systems and its effect on floating chamber measurements. *Limnology and Oceanography* 55: 1723–1732.

Vaz, L., Frankenbach, S., Serôdio, J., Dias, J.M. 2019. New insights about the primary production dependence on abiotic factors: Ria de Aveiro case study. *Ecological Indicators*: 106, 105555, ISSN 1470-160X, https://doi.org/10.1016/j.ecolind.2019.105555.

Wang, Z. A. and W.-J. Cai. 2004. Carbon dioxide degassing and inorganic carbon export from a marsh-dominated estuary (the Dublin River): a marsh CO_2 pump. *Limnology and Oceanography* 49: 341–354.

Wang, Z.A., K.D. Kroeger, N.K. Ganju, M.E. Gonneea, and S.N. Chu. 2016. Intertidal salt marshes as an important source of inorganic carbon to the coastal ocean. *Limnology and Oceanography* 61: 1916–1931. https://doi.org/10.1002/lno.10347.

Wang, S.R., D. Di Iorio, W.-J. Cai, and C.S. Hopkinson. 2018. Inorganic carbon and oxygen dynamics in a marsh-dominated estuary. *Limnology and Oceanography* 63: 47-71. https://doi.org/10.1002/lno.10614.

Wanninkhof, R. 1992. Relationship between gas exchange and wind speed over the ocean. *Journal of Geophysical Research* 97: 7373–7382.

Weiss, R.F. 1974. Carbon dioxide in water and seawater: the solubility of a non-ideal gas. *Marine Chemistry* 2: 203–215.

Yang C., Telmer K., and Veizer J. 1996. Chemical dynamics of the 'St. Lawrence' riverine system: δH2O, δ^{18}OH2O, δ^{13}CDIC, δ^{34}SSulfate, and Dissolved $^{87}Sr/^{86}Sr$. *Geochimica Cosmochimica Acta* 60: 851–866.

Yates, K. K., C. Dufore, N. Smiley, C. Jackson, and R. B. Halley. 2007. Diurnal variation of oxygen and carbonate system parameters in Tampa Bay and Florida Bay. *Marine Chemistry* 104: 110–124.

Zemmelink, H. J., H.A. Slagter, C. van Slooten, J. Snoek, B. Heusinkveld, J. Elbers, N.J. Bink, W. Klaassen, C. J. M. Philippart, and H. J. W. de Baar. 2009. Primary production and eddy correlation measurements of CO_2 exchange over an intertidal estuary. *Geophysical Research Letters* 36: LI19606. https://doi.org/10.1029/2009GL039285.

Zhang, L., M. Xue, and Q. Liu. 2012. Distribution and seasonal variation in the partial pressure of CO_2 during autumn and winter in Jiaozhou Bay, a region of high urbanization. *Marine Pollution Bulletin* 64: 56–65.

Figure/Table captions

Table 1 Inorganic carbon parameters measured during eight 24 hour-cycles to six 24h and two 12h cycles in the Arcachon flat (44°42.400'N 01°07.500'W) (number of values, mean ± standard deviation in bold and range between brackets). T and S water temperature and salinity, δ^{13}C-DIC dissolved inorganic carbon isotopic ratio, TA total alkalinity, pCO_2 partial pressure of CO_2, and DIC dissolved inorganic carbon. DIC were estimated from measured salinity, temperature, TA and pCO_2 values using the CO_2 system calculation program (Lewis and Wallace 1998) parameterized with the carbonic acid constants sets proposed by Mehrbach et al. (1973) refitted by Dickson and Millero (1987), the borate acidity constant from Lee et al. (2010) and the CO_2 solubility coefficient of Weiss (1974). 15/04/2008 10:00:00 (TU) – 16/04/2008 10:00:00, 02/07/2008 10:00 – 03/07/2008 10:00, 18/09/2008 11:00 – 19/09/2008 11:00, 06/11/2008 08:00 – 06/11/2008 17:00, 29/01/2009 06:00 – 29/01/2009 14:00, 15/04/2009 13:00 – 16/04/2009 13:00, 25/06/2009 06:00 – 26/06/2009 06:00 and 04/09/2009 05:00 – 05/09/2009 05:00. Notice that November 2008 and January 2009 were 12 hour-cycles

Table 2 Gas transfer velocities (k_{600}) and air-sea CO_2 fluxes computed at high tide day and night periods (Fig. 3, the four-hour emerged-periods around low tide at each cycle were removed) for each cycle in the Arcachon flat (mean ± standard deviation and range between brackets). U_{10} values were computed from wind speed values measured at 9 meters high by the Lège-Cap Ferret Meteo-France station, 12 km far from the 24-H site) using the Amorocho and

DeVries (1980) equation. k_{600} values were estimated according to Wanninkhof et al. (1992), Raymond & Cole (2001) and Abril et al. (2009) equations (W92, RC01 and A09, respectively, see M&M). Air-sea CO_2 fluxes were then calculated from k_{600}, water and air pCO_2 values. A mean air pCO_2 value of 390 ppm was chosen according to Eddy Covariance (EC) measurements deployed at 1.8 km far from the tidal creek in 2008 and 2009 (Polsenaere et al. 2012a). For comparison, U_{10} and air-sea CO_2 flux values obtained in July 2008 from simultaneous EC measurements (Polsenaere et al. 2012a) in July 2008 are shown in red. No k_{600} calculations were attempted from these simultaneous EC flux and water pCO_2 measurements at this season due to strong spatial heterogeneity in water bodies highlighted in the present study (see Discussion section 4.4.2.)

Table 3 Seasonal, tidal and diurnal pCO_2 and water-atmosphere variation comparisons across tidal flat, bay, marsh-estuary and mangrove systems of the coastal zone ([a]diurnal and/or tidal, [b]spatial and/or longitudinal sampling methodology)

Table 4 Comparison between day and night pCO_2 values averaged over a same salinity range according to tidal phases (flooding/ebbing) for each 2008-2009 cycle. The non-parametric Mann-Whitney (p-values: *** = 0.0002; **** < 0.0001) test was used. / symbol indicates cycles (flooding and/or ebbing periods) where comparisons were not possible due to not enough data (no data > 5 min. with no significant salinity value difference between day and night periods). To the contrary, time periods (min.) (> 5 min.) where comparisons were possible are specified for each cycle. Temperature comparisons are also given along with the pCO_2 increase or decrease only due to day through nighttime temperature difference (calculated with the CO_2 System Calculation program (version 2.1.) (Lewis and Wallace 1998) from constant T, S, TA and DIC values measured during each cycle (see Table 1 and M&M section)

Fig. 1 Localization of the 24 hour-cycle site. (a) The Arcachon lagoon with the subtidal zone (channels and creeks) and the intertidal mudflat area; (b) the 24 hour-cycle site (24H, 44°42.400'N 01°07.500'W in the subtidal creek always immersed); the EC station (EC, 44°42.9858'N 01°08.6160'W, 1.8 km far from the 24-H site, in the intertidal area emerged for approximately four hours and immersed for approximately nine hours, Polsenaere et al. 2012a); the meteo-france station (A) (MF, 44°37.900'N 01°14.900W, 12.450 km far from the 24-H site). The *Zostera noltei* seagrass meadow is derived from the SPOT image of the 22 June 2005; it occupies 60 % of the intertidal area (shades of green show the differences in seagrass density, brown and yellow represent muddy and sandy areas)

Fig. 2 *In situ* water temperatures (dashed black curve), pCO_2 (black curve with black dots) and derived temperature-normalized pCO_2 ($NpCO_2$, i.e. pCO_2 variations due to biological activity or non-temperature effects, black dotted curve with empty black dots, annual mean temperature over 2008/09 17.7 ± 4.2°C, dotted line) and thermally forced seasonal pCO_2 according to Takahashi et al. (2002) ($TpCO_2$, i.e. pCO_2 variations due to thermal effects, grey dotted curve with grey dots, annual mean temperature over 2008/09, 17.7 ± 4.2°C, dotted line and pCO_2 496 ± 36 ppmv, dashed line); mean temperature and pCO_2 over the whole 2008 and 2009 period were chosen for $NpCO_2$ and $TpCO_2$ computations due to sampled cycle strategy and for better consistency in year comparisons. Minimum and maximum pCO_2 values (associated to the mean pCO_2 value) measured during each tidal cycle are also represented (vertical black lines)

Fig. 3 Tidal and diurnal variations in inorganic carbon and associated parameters measured during eight 24 hour-cycles to six 24h and two 12h cycles in the Arcachon flat. Water height (H), salinity (S), temperature (T), partial pressure of CO_2 in the water (pCO_2), total alkalinity

(TA), dissolved inorganic carbon (DIC) and dissolved inorganic carbon isotopic ratio (δ^{13}C-DIC); (a) 15/04/2008 10:00:00 (TU) – 16/04/2008 10:00:00, (b) 02/07/2008 10:00 – 03/07/2008 10:00, (c) 18/09/2008 11:00 – 19/09/2008 11:00, (d) 06/11/2008 08:00 – 06/11/2008 17:00, (e) 29/01/2009 06:00 – 29/01/2009 14:00, (f) 15/04/2009 13:00 – 16/04/2009 13:00, (g) 25/06/2009 06:00 – 26/06/2009 06:00 and (h) 04/09/2009 05:00 – 05/09/2009 05:00. T and S were measured every minute by the YSI multiparameter probe on board and H was measured every hour by the SHOM. The other parameters were sampled on board every hour. Clear and grey areas represent daytime and nighttime periods, respectively. Notice the same y-axis scale between cycles was chosen to better see seasonal variations and that November 2008 and January 2009 were 12 hour-cycles

Fig. 4 Cross-correlation plots of TA (a), DIC (c) and δ^{13}C-DIC (d) values versus salinity and apparent 0 end-member versus *in situ* catchment TA value comparison (b). TA versus S slopes are all significantly positive, DIC versus S slopes are significantly positive except in September 2009 (negative); and δ^{13}C-DIC versus S slopes are positive and significant except in April 2008, November 2008, September 2009. (b) Apparent 0 end-member TA and *in situ* catchment TA correspond to Y-intercept of TA versus S cross-correlations and *in situ* TA measurements carried out at the same time over the Arcachon lagoon watershed watercourses (see Polsenaere et al. 2012b) computed here as discharge-weighted TA means, respectively

Fig. 5 Diurnal/tidal plots of water temperature and pCO_2 versus salinity for the four periods: HT_N high tide at night (dark blue triangle), LT_N low tide at night (green inversed triangle), LT_D low tide at day (yellow inversed triangle) and HT_D high tide at day (clear blue triangle). (a, b) April 2008, (c, d) July 2008, (e, f) September 2008, (g, h) November 2008, (I, j) January 2009, (k, l) April 2009, (m, n) June 2009 and (o, p) September 2009. Notice the same y-axis

pCO_2 scale between all cycles was chosen to better observe diurnal and tidal variations. The same x-axis temperature and salinity scales between April 2008-2009, July 2008-June 2009 and September 2008-2009 were also chosen to better observe variations during the same seasons from 2008 to 2009

Table 1

	T (°C)	*S*	δ^{13}C-DIC (‰)	TA (mmol kg^{-1})	pCO_2 (ppmv)	DIC (mmol kg^{-1})
April 2008	*1441*	*1441*	*23*	*25*	*1441*	*25*
	13.9 ± 0.6	**29.2 ± 0.6**	**-1.1 ± 1.1**	**2.081 ± 0.028**	**474 ± 14**	**1.948 ± 0.024**
	(12.8 ~ 15.4)	(26.2 ~ 30.1)	(-3.7 ~ -0.4)	(2.000 ~ 2.119)	(442 ~ 496)	(1.884 ~ 1.985)
July 2008	*1464*	*1464*	*24*	*25*	*1434*	*25*
	22.2 ± 0.6	**31.2 ± 0.6**	**-0.5 ± 0.4**	**2.131 ± 0.035**	**461 ± 14**	**1.926 ± 0.028**
	(21.2 ~ 23.4)	(30.2 ~ 32.6)	(-1.7 ~ 0.2)	(2.072 ~ 2.211)	(432 ~ 499)	(1.879 ~ 1.995)
September 2008	*1428*	*1428*	*25*	*25*	*1436*	*25*
	19.2 ± 0.2	**33.6 ± 0.3**	**-0.6 ± 0.3**	**2.255 ± 0.021**	**515 ± 36**	**2.062 ± 0.017**
	(18.8 ~ 20.2)	(33.1 ~ 34.5)	(-1.5 ~ -0.1)	(2.223 ~ 2.301)	(405 ~ 597)	(2.017 ~ 2.086)
November 2008	*541*	*541*	*10*	*10*	*541*	*10*
	12.3 ± 0.2	**32.2 ± 0.3**	**-0.6 ± 0.3**	**2.202 ± 0.020**	**463 ± 19**	**2.050 ± 0.022**
	(12.0 ~ 12.6)	(31.8 ~ 32.6)	(-1.3 ~ -0.3)	(2.180 ~ 2.234)	(419 ~ 497)	(2.021 ~ 2.081)
January 2009	*490*	*480*	*9*	*9*	*480*	*9*
	8.9 ± 0.4	**23.2 ± 1.5**	**-1.0 ± 0.5**	**1.646 ± 0.086**	**480 ± 15**	**1.594 ± 0.076**
	(8.3 ~ 10.3)	(20.4 ~ 25.6)	(-2.1 ~ -0.5)	(1.493 ~ 1.733)	(452 ~ 503)	(1.458 ~ 1.669)
April 2009	*1518*	*1518*	*25*	*25*	*1518*	*25*
	13.7 ± 0.3	**30.1 ± 1.0**	**-0.7 ± 0.1**	**2.006 ± 0.053**	**525 ± 14**	**1.891 ± 0.045**
	(12.7 ~ 14.5)	(24.8 ~ 31.5)	(-0.9 ~ -0.5)	(1.840 ~ 2.101)	(494 ~ 568)	(1.752 ~ 1.968)
June 2009	*1441*	*1441*	*24*	*25*	*1441*	*25*
	21.5 ± 0.6	**31.0 ± 0.4**	**-0.2 ± 0.2**	**2.099 ± 0.029**	**490 ± 27**	**1.916 ± 0.023**
	(20.0 ~ 23.3)	(30.2 ~ 32.2)	(-0.4 ~ 0.2)	(2.044 ~ 2.156)	(419 ~ 545)	(1.866 ~ 1.951)
September 2009	*1441*	*1440*	*25*	*25*	*1435*	*25*
	20.9 ± 0.3	**34.0 ± 0.3**	**-0.2 ± 0.3**	**2.218 ± 0.020**	**530 ± 39**	**2.021 ± 0.021**
	(20.2 ~ 21.5)	(33.5 ~ 34.8)	(-0.90 ~ 0.4)	(2.187 ~ 2.251)	(453 ~ 601)	(1.978 ~ 2.051)
2008-2009 Average	*9764*	*9753*	*165*	*169*	*9726*	*169*
	17.7 ± 4.2	**30.5 ± 3.4**	**-0.6 ± 0.4**	**2.079 ± 0.036**	**496 ± 36**	**1.926 ± 0.032**
	(8.3 ~ 23.4)	(20.4 ~ 34.8)	(-3.7 ~ 0.4)	(1.493 ~ 2.301)	(405 ~ 601)	(1.458 ~ 2.086)

Table 2

		U_{10} (m s^{-1})	K_{600} (cm h^{-1})			Air-Sea CO_2 fluxes (mmol m^{-2} h^{-1})		
			W92	RC01	A09	W92	RC01	A09
Apr. 08	*Day*	**4.42 ± 1.42** (2.02 ~ 6.06)	**6.59 ± 3.71** (1.26 ~ 11.37)	**9.9 ± 4.46** (3.87 ~ 15.91)	**17.04 ± 4.92** (8.76 ~ 22.74)	**0.19 ± 0.1** (0.05 ~ 0.34)	**0.29 ± 0.12** (0.14 ~ 0.48)	**0.5 ± 0.12** (0.32 ~ 0.69)
	Night	**2.88 ± 0.7** (2.02 ~ 4.04)	**2.71 ± 1.27** (1.26 ~ 5.05)	**5.38 ± 1.34** (3.87 ~ 7.85)	**11.74 ± 2.4** (8.76 ~ 15.72)	**0.07 ± 0.04** (0.02 ~ 0.14)	**0.13 ± 0.05** (0.07 ~ 0.22)	**0.29 ± 0.11** (0.16 ~ 0.44)
Jul. 08	*Day*	**4.46 ± 2.34** (2.02 ~ 11.1)	**7.71 ± 9.88** (1.26 ~ 38.21)	**14.92 ± 24.73** (3.87 ~ 93.05)	**17.16 ± 8.06** (8.69 ~ 40.09)	**0.18 ± 0.23** (0.03 ~ 0.9)	**0.36 ± 0.58** (0.09 ~ 2.19)	**0.41 ± 0.2** (0.2 ~ 0.94)
	Night	**5.05 ± 1.43** (3.03 ~ 6.06)	**8.37 ± 4.03** (2.84 ~ 11.37)	**12.12 ± 4.94** (5.51 ~ 15.91)	**19.2 ± 4.91** (12.24 ~ 22.68)	**0.21 ± 0.11** (0.07 ~ 0.31)	**0.31 ± 0.13** (0.14 ~ 0.43)	**0.49 ± 0.13** (0.32 ~ 0.61)
EC data Tidal flat	*Day*	**3.86 ± 1.29** (1.29 ~ 7.71)				**-2.25 ± 2.7** (-12.38 ~ 2.1)		
	Night	**4.3 ± 2.21** (0.69 ~ 10.14)				**0.12 ± 1.37** (-2.56 ~ 1.76)		
Sep. 08	*Day*	**2.48 ± 0.83** (1.01 ~ 4.04)	**2.1 ± 1.33** (0.32 ~ 5.05)	**4.72 ± 1.41** (2.72 ~ 7.85)	**10.32 ± 2.86** (5.24 ~ 15.73)	**0.08 ± 0.05** (0.01 ~ 0.16)	**0.19 ± 0.06** (0.1 ~ 0.3)	**0.42 ± 0.15** (0.2 ~ 0.68)
	Night	**2.31 ± 1.39** (1.01 ~ 5.05)	**2.17 ± 2.66** (0.32 ~ 7.9)	**4.82 ± 2.95** (2.72 ~ 11.17)	**9.76 ± 4.81** (5.29 ~ 19.22)	**0.08 ± 0.11** (0.01 ~ 0.32)	**0.19 ± 0.12** (0.09 ~ 0.45)	**0.38 ± 0.19** (0.2 ~ 0.78)
Nov. 08	*Day*	**7.74 ± 1.77** (5.05 ~ 10.09)	**19.37 ± 8.37** (7.9 ~ 31.58)	**33.33 ± 19.51** (11.17 ~ 65.36)	**28.38 ± 6.12** (19.08 ~ 36.54)	**0.53 ± 0.22** (0.25 ~ 0.87)	**0.92 ± 0.52** (0.36 ~ 1.81)	**0.79 ± 0.14** (0.61 ~ 1.01)
	Night							
Jan. 09	*Day*	**2.27 ± 0.97** (1.01 ~ 3.03)	**1.82 ± 1.25** (0.32 ~ 2.84)	**4.4 ± 1.36** (2.72 ~ 5.51)	**9.58 ± 3.3** (5.27 ~ 12.19)	**0.06 ± 0.04** (0.01 ~ 0.11)	**0.14 ± 0.06** (0.08 ~ 0.21)	**0.29 ± 0.13** (0.16 ~ 0.46)
	Night							
Apr. 09	*Day*	**5.35 ± 3.37** (1.01 ~ 10.09)	**12.03 ± 12.55** (0.32 ~ 31.58)	**22.84 ± 25.61** (2.72 ~ 65.36)	**20.02 ± 11.43** (5.24 ~ 36.09)	**0.56 ± 0.59** (0.01 ~ 1.59)	**1.06 ± 1.2** (0.12 ~ 3.3)	**0.93 ± 0.55** (0.23 ~ 1.82)
	Night	**4.04 ± 1.81** (2.02 ~ 7.07)	**5.9 ± 5.23** (1.26 ~ 15.48)	**9.43 ± 6.95** (3.87 ~ 22.65)	**15.58 ± 6.18** (8.65 ~ 25.9)	**0.23 ± 0.2** (0.06 ~ 0.6)	**0.38 ± 0.26** (0.18 ~ 0.87)	**0.63 ± 0.21** (0.4 ~ 1)
Jun. 09	*Day*	**3.62 ± 1.32** (1.01 ~ 5.05)	**4.55 ± 2.65** (0.32 ~ 7.9)	**7.39 ± 2.92** (2.72 ~ 11.17)	**14.18 ± 4.51** (5.25 ~ 19.06)	**0.13 ± 0.08** (0.01 ~ 0.25)	**0.22 ± 0.09** (0.09 ~ 0.35)	**0.43 ± 0.14** (0.17 ~ 0.6)
	Night	**3.7 ± 1.17** (3.03 ~ 5.05)	**4.53 ± 2.92** (2.84 ~ 7.9)	**7.4 ± 3.27** (5.51 ~ 11.17)	**14.54 ± 4.02** (12.21 ~ 19.18)	**0.12 ± 0.08** (0.07 ~ 0.22)	**0.2 ± 0.09** (0.13 ~ 0.31)	**0.4 ± 0.12** (0.29 ~ 0.53)
Sep. 09	*Day*	**9.31 ± 3.1** (5.05 ~ 13.12)	**29.51 ± 18.64** (7.9 ~ 53.37)	**81.73 ± 80.78** (11.17 ~ 188.61)	**32.09 ± 10.07** (19.18 ~ 46.85)	**1.02 ± 0.65** (0.23 ~ 1.83)	**2.8 ± 2.68** (0.32 ~ 6.48)	**1.11 ± 0.47** (0.48 ~ 1.65)
	Night	**2.88 ± 0.91** (2.02 ~ 4.04)	**2.8 ± 1.7** (1.26 ~ 5.05)	**5.48 ± 1.78** (3.87 ~ 7.85)	**11.71 ± 3.14** (8.71 ~ 15.75)	**0.11 ± 0.06** (0.05 ~ 0.21)	**0.23 ± 0.06** (0.14 ~ 0.33)	**0.49 ± 0.11** (0.32 ~ 0.66)

Table 3

Study Site	Seasonal pCO_2 range (ppmv)	Diurnal-tidal pCO_2 range (ppmv)	Water-atmosphere CO_2 flux (mmol m^{-2} h^{-1})	Reference
Arcachon tidal flat (France)	461 ± 14 (July 2008) – 530 ± 39 (September 2009)	(452 - 503) (January 2009) to (405 - 597) (September 2008)	0.27 ± 0.22 to 0.56 ± 0.54	This study[a]
Aiguillon tidal flat (France)	(390 - 609) (spring - summer 2017) (215 - 1929) (summer - fall 2018)		0.14 (-0.075 to 1.13, summer - winter)	Polsenaere et al. (2018)[b]; Coignot et al. (2020; in prep.)[b]
Aiguillon tidal flat (France)		(466 - 1024) (HT-LT) (summer 2018)	1.00 ± 0.82	Ternon et al. (2018)[a]
Duplin River salt marsh-estuary (Georgia, USA)		(500 - 4000) (HT-LT, winter) to (1600 - 12,000) (HT-LT, summer) (2014)	-0.7 to -5.5 and -0.6 to -3.9	Wang et al. (2018)[a,b]
Tidal marsh channel of the Fier d'Ars (Ré Island, France)	385 ± 60 (267 - 522) (summer) to 460 ± 58 (334 - 569) (autumn)	(377 - 510) (HT-LT, winter 2018) to (334 - 569) (HT - LT, Autumn 2018)	-0.18 ± 0.18 (spring) to 0.10 ± 0.08 (winter)	Mayen et al. (in prep.)[a]
Amazon estuary - tidal forest channel		5000 ± 300 - 2320 ± 40 (LT - HT, February 2007)		Abril et al. (2013)[a]
Ras Dege (Tanzania) mangrove creek		500 - 5000 (September 2005)	0.04-3.33	Bouillon et al. (2007)[a]
Nagada (Papua New Guinea) and the Gaderu (India) mangrove creeks		(540 - 1680) and (1380 - 4770) (July, August 2000)	1.82 ± 1.38 and 2.33 ± 4.20	Borges et al. (2003)[a]
Bay of Brest (subtidal)	200 - 700 (summer-winter, 2013 to 2010)		-0.0083 to -0.38 (spring and summer) and 0.038 to 0.91 (fall and winter)	Bozec et al. (2011)[a]
Estuary of Guadalquivir Estuary and the Bay of Cadiz	341 ± 18 (February 2007) - 411 ± 20 (November 2006)		-0.058 (February 2007) and 0.15 (November 2006)	Ribas-Ribas et al. (2011)[b]
Coastal systems of Cadiz Bay (Spain)		(589 - 1244), (525 - 1405) and (742 - 1059) (HT-LT, summer 2015)	0.375 to 2.37	Burgos et al. (2018)[a,b]
Jiaozhou Bay (East China Sea)	315 - 720 (autumn 2007) and 145 - 315 (winter 2008)		0.12 (autumn) and -0.68 (winter)	Zhang et al. (2012)[b]
Tampa and Florida bays (US)	414 ± 86 (October 2003); 351 ± 72 (March 2000)	(262 - 580) (October 2003); (260 - 497) (March 2000)		Yates et al. (2007)[a]
Macrophyte meadow (Baltic Sea)		281 ± 88 (July); 219 ± 24 (August); 1488 ± 574 (September 2011)		Saderne et al. (2013)[a]
Zostera marina meadow, Eastern shore of Virginia (US)	425 (April) - 490 (June 2015)	(193 - 731) (April); (256 - 859) (June 2015)		Berg et al. (2019)[a]
Guanabara Bay (Brazil)	353 ± 141 and 194 ± 127 (S3); 380 ± 286 and 203 ± 159 (S4); 364 ± 343 and 132 ± 74 (S5) (winter and summer)	591 ± 231 to 194 ± 114 (September 2013); 163 ± 40 to 116 ± 25 (January 2014); 346 ± 166 to 146 ± 106 (February 2014); 637 ± 421 to 265 ± 186 (April 2014) (S4, S5)	-2.87 (S3); -2.16 (S4); -2.52 (S5)	Cotovicz et al. (2015)[a,b]

Table 4

		Day			Night			Significant differences (Day vs Night)			pCO_2 increase or decrease only due to day through night T difference
		Salinity	pCO_2 (ppmv)	T (°C)	Salinity	pCO_2 (ppmv)	T (°C)	Salinity	pCO_2	T	
Apr. 2008	**Flooding**	/	/		/	/		/	/	/	/
	Ebbing (30 min.)	29.27	481	14.47	29.27	471	13.56	No	Yes ****	Yes ****	-18
Jul. 2008	**Flooding**	/	/		/	/		/	/	/	/
	Ebbing (10 min.)	30.4	493	21.35	30.43	471	22.55	No	Yes ****	Yes ****	+21
Sept. 2008	**Flooding (120 min.)**	33.55	513	18.95	33.55	537	19.07	No	Yes ****	Yes ****	+2
	Ebbing	/	/		/	/		/	/	/	/
Nov. 2008	**Flooding**	/	/		/	/		/	/	/	/
	Ebbing	/	/		/	/		/	/	/	/
Jan. 2009	**Flooding**	/	/		/	/		/	/	/	/
	Ebbing	/	/		/	/		/	/	/	/
Apr. 2009	**Flooding**	/	/		/	/		/	/	/	/
	Ebbing	/	/		/	/		/	/	/	/
Jun. 2009	**Ebbing**	/	/		/	/		/	/	/	/
	Flooding	/	/		/	/		/	/	/	/
Sept. 2009	**Flooding (30 min.)**	33.89	552	20.97	33.9	572	20.58	No	Yes ***	Yes ****	-8
	Ebbing (15 min.)	33.97	540	20.97	33.96	535	20.84	No	Yes ***	Yes ****	-3

Fig. 1

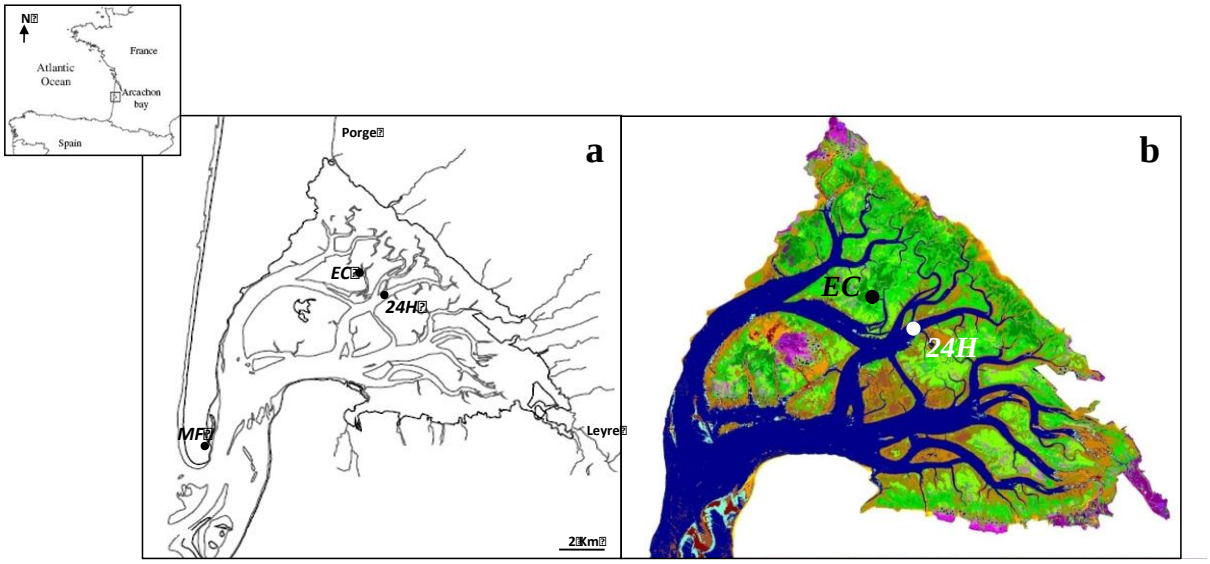
N
France
Atlantic Ocean
Arcachon bay
Spain
Porge
a
EC
24H
MF
Leyre
2 Km
b
EC
24H

Fig. 2

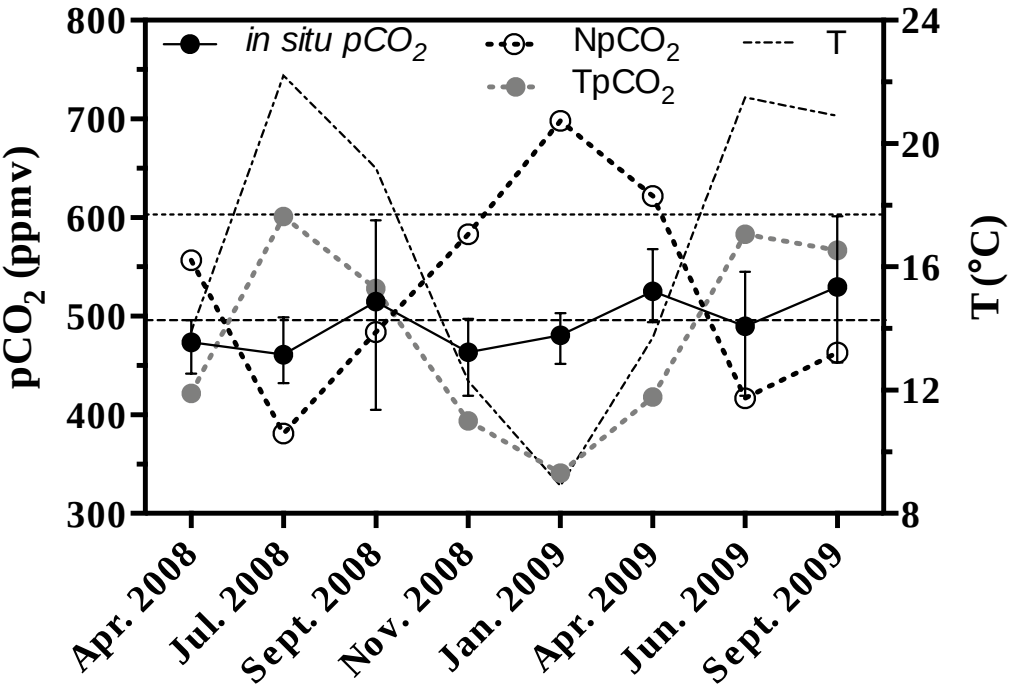
800
700
600
500
400
300
24
20
16
12
8
pCO2 (ppmv)
T (°C)
in situ pCO2
NpCO2
TpCO2
T
Apr. 2008
Jul. 2008
Sept. 2008
Nov. 2008
Jan. 2009
Apr. 2009
Jun. 2009
Sept. 2009

Fig. 3

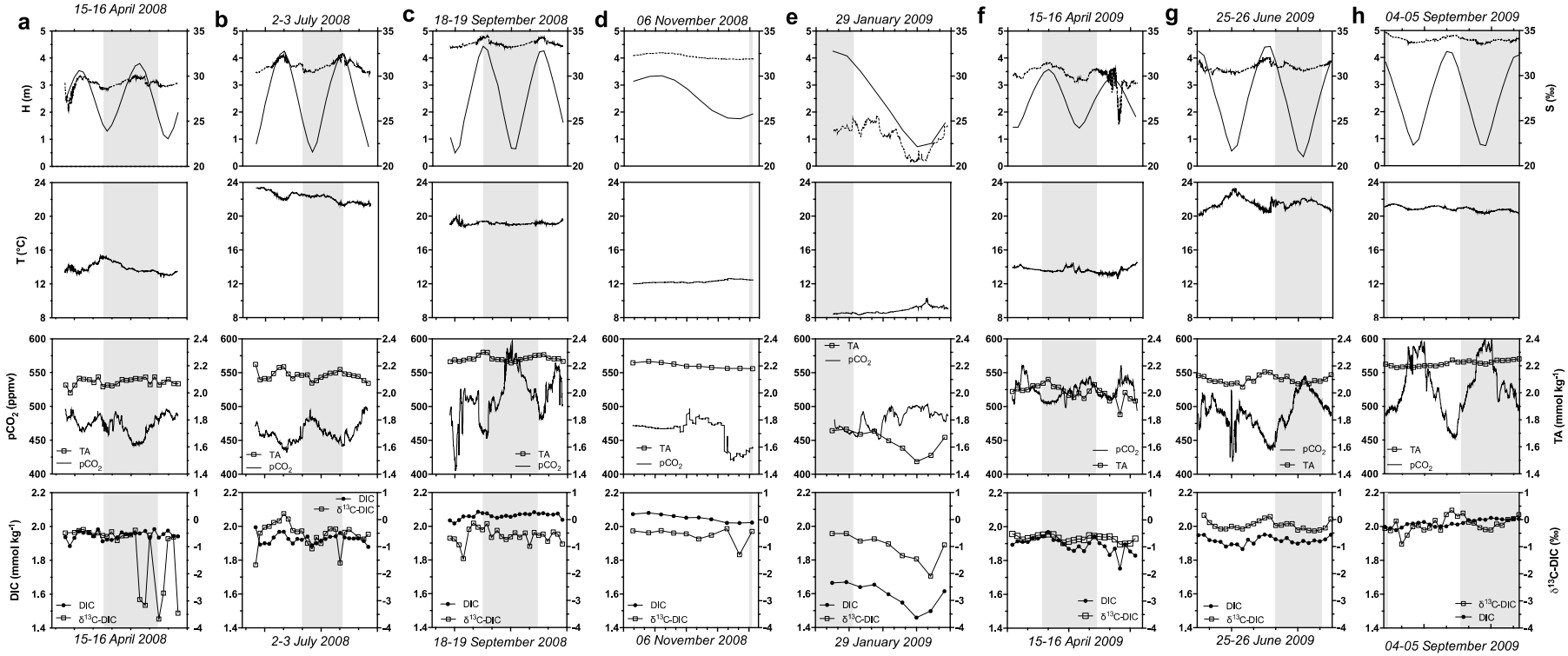
a
15-16 April 2008
b
2-3 July 2008
c
18-19 September 2008
d
06 November 2008
e
29 January 2009
f
15-16 April 2009
g
25-26 June 2009
h
04-05 September 2009
H (m)
S (‰)
T (°C)
pCO2 (ppmv)
TA (mmol kg-1)
DIC (mmol kg-1)
δ13C-DIC (‰)
TA
pCO2
DIC
δ13C-DIC

Fig. 4

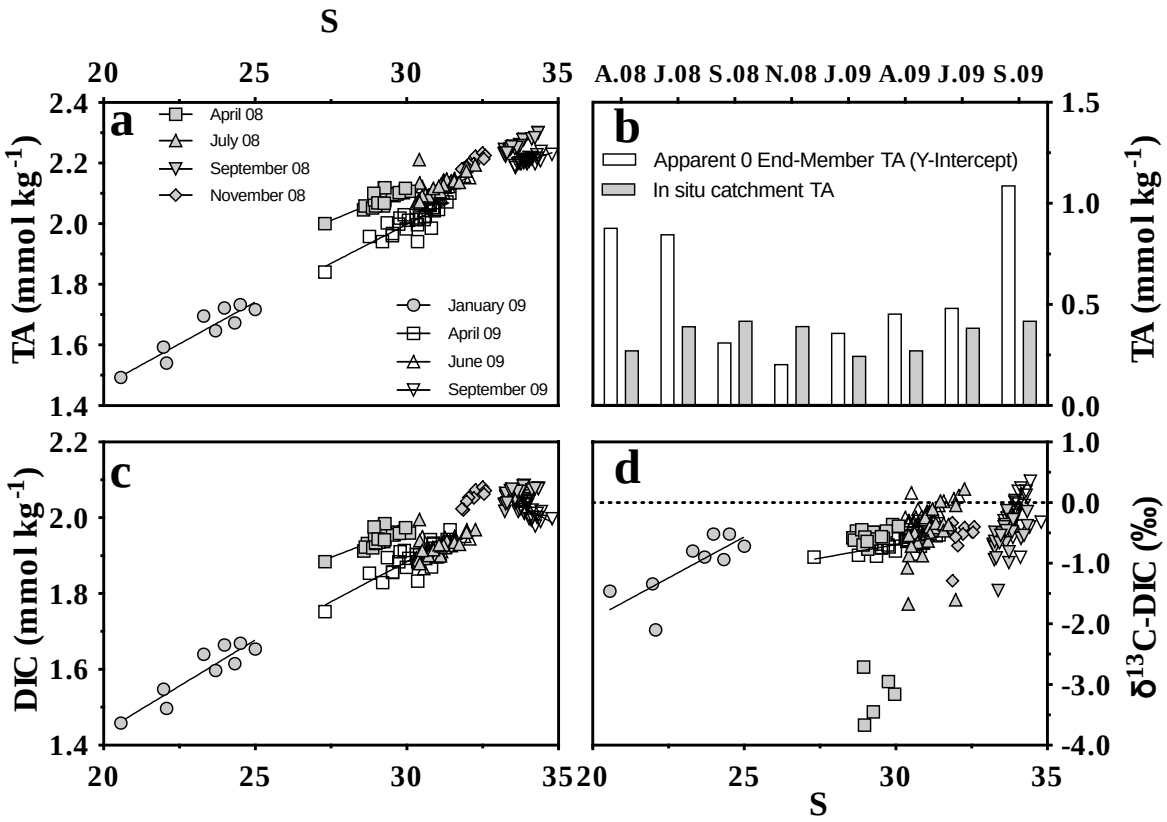
S
20
25
30
35
A.08 J.08 S.08 N.08 J.09 A.09 J.09 S.09
a
April 08
July 08
September 08
November 08
January 09
April 09
June 09
September 09
TA (mmol kg-1)
b
Apparent 0 End-Member TA (Y-Intercept)
In situ catchment TA
TA (mmol kg-1)
c
DIC (mmol kg-1)
d
δ13C-DIC (‰)
S

Fig. 5

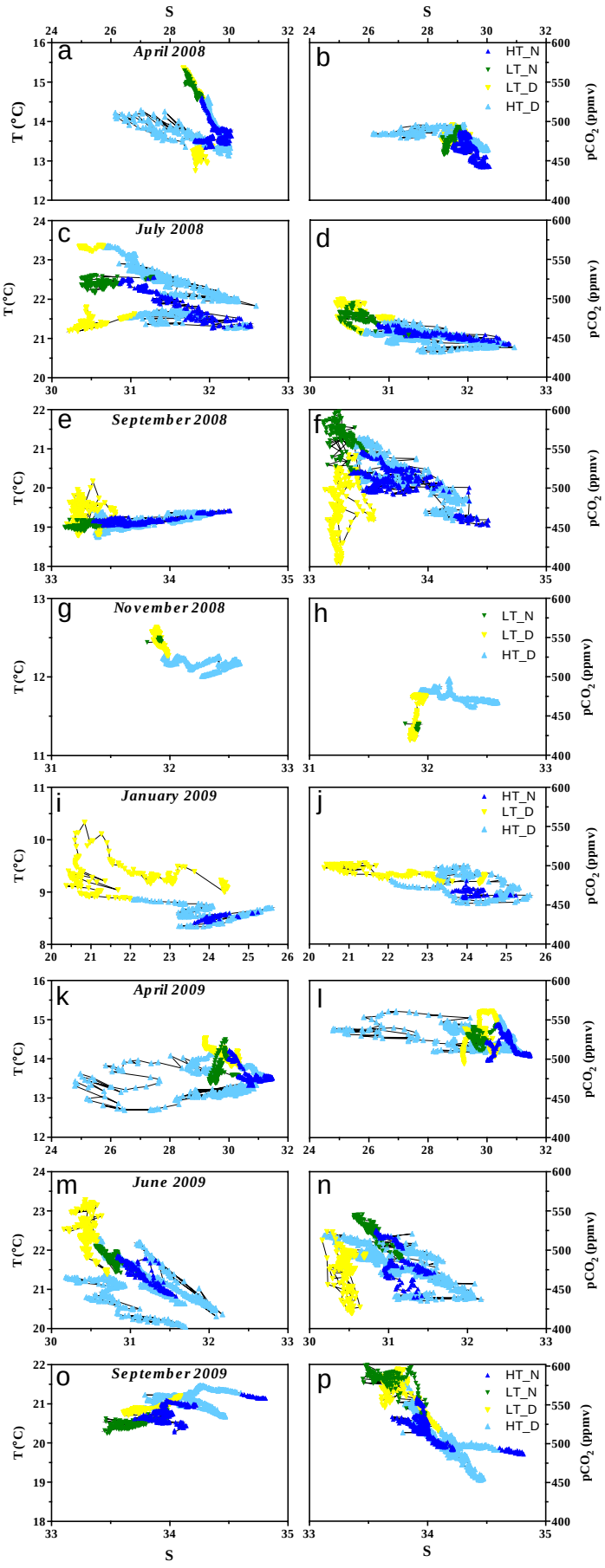
a
April 2008
b
HT_N
LT_N
LT_D
HT_D
c
July 2008
d
e
September 2008
f
g
November 2008
h
i
January 2009
j
k
April 2009
l
m
June 2009
n
o
September 2009
p
S
T (°C)
pCO2 (ppmv)